AD-A116 891 TEXAS UNIV AT AUSTIN APPLIED RESEARCH LABS F/G 20/1
A SUMMARY OF THE RESULTS OF A STUDY OF ACOUSTIC BOTTOM INTERACT--ETC(U)
JUN 82 R A KOCH N00014-78-C-0113
UNCLASSIFIED ARL-TR-82-30 NL

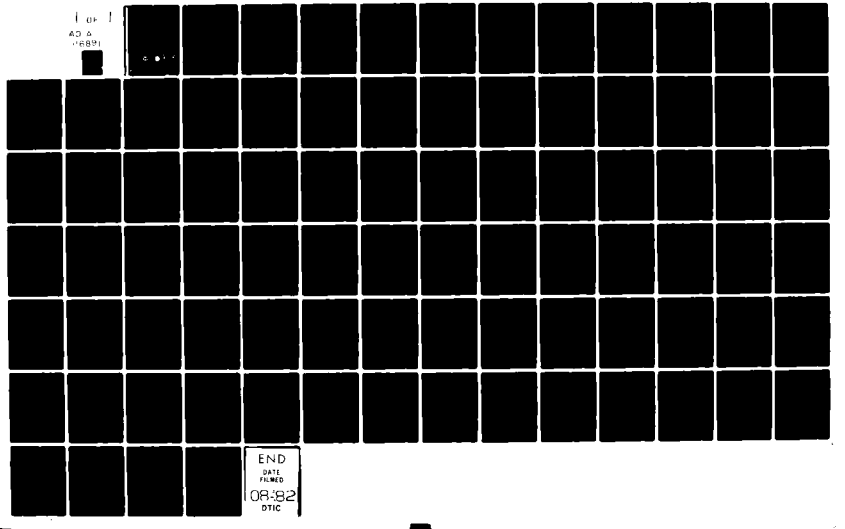

END
DATE FILMED
08-82
DTIC

(12)

ARL-TR-82-30

Copy No. 39

A SUMMARY OF THE RESULTS OF A STUDY OF ACOUSTIC BOTTOM INTERACTION IN A RANGE DEPENDENT ENVIRONMENT

Robert A. Koch

APPLIED RESEARCH LABORATORIES
THE UNIVERSITY OF TEXAS AT AUSTIN
POST OFFICE BOX 8029, AUSTIN, TEXAS 78712-8029

1 June 1982

Technical Report

APPROVED FOR PUBLIC RELEASE;
DISTRIBUTION UNLIMITED.

Prepared for:

NAVAL OCEAN RESEARCH AND
DEVELOPMENT ACTIVITY
DEPARTMENT OF THE NAVY
NSTL STATION, MS 39529

UNCLASSIFIED

SECURITY CLASSIFICATION OF THIS PAGE *(When Data Entered)*

REPORT DOCUMENTATION PAGE	READ INSTRUCTIONS BEFORE COMPLETING FORM
1. REPORT NUMBER	2. GOVT ACCESSION NO. 3. RECIPIENT'S CATALOG NUMBER
4. TITLE *(and Subtitle)* A SUMMARY OF THE RESULTS OF A STUDY OF ACOUSTIC BOTTOM INTERACTION IN A RANGE DEPENDENT ENVIRONMENT	5. TYPE OF REPORT & PERIOD COVERED technical report
	6. PERFORMING ORG. REPORT NUMBER ARL-TR-82-30
7. AUTHOR*(s)* Robert A. Koch	8. CONTRACT OR GRANT NUMBER*(s)* N00014-78-C-0113
9. PERFORMING ORGANIZATION NAME AND ADDRESS Applied Research Laboratories The University of Texas at Austin Austin, TX 78712-8029	10. PROGRAM ELEMENT, PROJECT, TASK AREA & WORK UNIT NUMBERS
11. CONTROLLING OFFICE NAME AND ADDRESS Naval Ocean Research and Development Activity Department of the Navy NSTL Station, MS 39529	12. REPORT DATE 1 June 1982 13. NUMBER OF PAGES 80
14. MONITORING AGENCY NAME & ADDRESS*(if different from Controlling Office)*	15. SECURITY CLASS. *(of this report)* UNCLASSIFIED 15a. DECLASSIFICATION DOWNGRADING SCHEDULE

16. DISTRIBUTION STATEMENT *(of this Report)*

Approved for public release; distribution unlimited.

17. DISTRIBUTION STATEMENT *(of the abstract entered in Block 20, if different from Report)*

18. SUPPLEMENTARY NOTES

19. KEY WORDS *(Continue on reverse side if necessary and identify by block number)*

bottom interaction	sediment attenuation gradient
slope propagation	range variable
adiabatic normal mode	lateral variability
sediment type	energy partition
sediment attenuation	slope angle

20. ABSTRACT *(Continue on reverse side if necessary and identify by block number)*

This report summarizes the results of research carried out during 1981 at Applied Research Laboratories, The University of Texas at Austin (ARL:UT), on acoustic bottom interaction in a range variable environment. The major topic is adiabatic normal mode modeling of range variable environments involving slopes or lateral variation. In particular the study of slope propagation is extended to consider sediment type, sediment attenuation gradients, an analysis of energy partitioning, and a reexamination of slope angle effects. The study of lateral variability

DD FORM 1 JAN 73 1473 EDITION OF 1 NOV 65 IS OBSOLETE

UNCLASSIFIED

SECURITY CLASSIFICATION OF THIS PAGE *(When Data Entered)*

20. (cont'd)
considers an absorbing patch problem and its relation to province descriptions of range variable environments. The sensitivity of propagation over slopes to lateral variation of sediment type is also considered.

TABLE OF CONTENTS

LIST OF FIGURES

I. INTRODUCTION

This report presents the results of a 1981 study of bottom interaction in a range changing environment conducted at Applied Research Laboratories, The University of Texas at Austin (ARL:UT). Bottom interaction in a range variable environment is one of the major areas of study in the ARL:UT bottom interaction program. The main thrust of this work has been to determine the effects and relative importance of subbottom variability and sloping boundaries on the propagation of low frequency underwater sound.

To adequately characterize propagation in range variable environments, we must consider the effects of the environment on the acoustic signal relevant to a given problem. A suitable indicator of the effects must be chosen and an appropriate description of the environment must be employed. These considerations may be problem dependent.

One example of the problems in propagation through range variable environments is the determination of noise field characteristics given some configuration of sources. This is the simplest such problem because the components of the noise field have random phase, so that only the incoherent (phase averaged) sound field is relevant. The phase content of an acoustic signal might be quite sensitive to environmental details whereas the amplitude of a noise field will be determined by gross features of the environment. Thus the incoherent propagation loss is a suitable indicator of environmental effects on noise fields. Likewise the extent to which gross environmental features must be specified is then an important consideration in implementing a range variable environmental description and will determine the type of acoustic propagation model required.

Except for mode cutoff considerations or effects outside the adiabatic model, such as mode coupling, the intermediate environment between source and receiver does not play a primary role, other than through attenuation, in adiabatic normal mode analysis of noise propagation. This is because in the adiabatic model the depth dependence for each mode is a locally defined quantity determined by the local sound velocity profile (SVP), water depth, and geoacoustic description. The range dependent amplitude for each mode has a phase which is dependent upon the intermediate environment between the receiver and each noise but which is random with respect to any of the other contributing sources. These various sources contribute through a given mode to the intensity at the receiver and therefore an average intensity is produced which is the incoherent sum of the intensity for that mode from each noise source. The intensity of each mode varies with range due to cylindrical spreading, attenuation, and variation of the local mode function. Cylindrical spreading loss is independent of the intermediate environment except for its extent. The attenuation through the intermediate environment is cumulative but does not affect the depth dependence of the mode functions at the receiver.

The method used to describe range variability must also be examined. One wants to avoid the expense of numerous detailed measurements of acoustic properties while still maintaining a predictive capability. Several procedures use geological information and available measurements to produce geoacoustic profiles. One such procedure is to construct local geoacoustic parameter sets by suitably interpreting acoustic transmission measurements and cores taken in a given area. Another possibility is to use available geological information to define geophysical provinces characterized by particular sediment types, etc., with corresponding averaged geoacoustic parameters. In practice these two methods are combined.

The first ARL:UT work on range variability in 1978 was primarily an assessment of analytical tools for describing sound propagation in a range variable environment. Also begun was a determination of the

importance of lateral subbottom variability and sloping boundaries. The FY 78 work is summarized in Ref. 1.

In 1979 the range variable work included several accomplishments. In 1978 coupled mode theory[2,3] was determined to be the best means for modeling and investigating bottom interaction mechanisms in a range variable environment, and a firm theoretical foundation was established for the application of coupled mode theory to problems of interest. One particular problem investigated was the effect of boundary condition approximations on coupled mode theory in sloping bottom problems.[4,5] The implications of the adiabatic approximation[6] were also studied and the 1978 work, concerning the importance of lateral variability and sloping boundaries, was continued. Another aspect of the 1979 work was the development of an adiabatic normal mode model. All the 1979 bottom interaction work is summarized in Ref. 8.

In 1980 the adiabatic normal mode model was used to examine the sensitivity of propagation over a sloping bottom to sediment attenuation.[9] This work demonstrated that spreading loss, renormalization loss, bottom attenuation, differential mode excitation, and mode cutoff are the basic mechanisms of acoustic slope propagation. Reference 9 also contains a theoretical development of the mathematical formalism for implementing coupled mode theory. A summary of this 1980 bottom interaction work is in Ref. 10.

Section II of this report gives the results of a study of sensitivity of upslope and downslope propagation to sediment type using incoherent propagation loss as an indicator. Section III presents the results of a sensitivity study on propagation over an absorbing patch and examines the merits of an averaged versus more detailed description of range variable environments. Portions of this work were performed in 1980 but were not discussed in Ref. 9. Section IV discusses the application of the results of Sections II and III to the combined problem of lateral variability over a sloping bottom. Section V summarizes the work and offers some observations.

II. A STUDY OF SLOPE PROPAGATION DEPENDENCE ON BOTTOM TYPE

In the study of the importance of sediment type on the sensitivity of propagation to attenuation precedence continues to be given to the identification of mechanisms rather than details that depend upon the specific realization used in the model. Thus this work addresses the relative importance of the previously identified slope propagation mechanisms for different sediment types and how this is reflected in propagation sensitivity to sediment attenuation.

A. The Model

The modeling tool used to make this investigation was the adiabatic *normal mode model*.[9] The downslope and upslope propagation geometries are shown in Figs. 1 and 2. The source position is at r=0 and $z=z_o$, and the bathymetric variation with constant slope occurs between r_1 = 40 km and r_2. Between r=0 and r_1 is a range invariant region, as is the region between r_2 and $r_3 = r_2 + 40$ km. The value of r_2 is determined by the slope angle and is 66.7 km or 120 km for a 3^o or 1^o slope, respectively. This arrangement of fixed length for the range invariant regions was chosen so that the comparisons between 1^o and 3^o slopes would only be affected by the difference in slope and in the horizontal extent of the sloping region (see Sections II.B.3 and II.C.3).

The water sound velocity profile (SVP) given in Fig. 3 was used throughout the region r=0 to $r=r_3$. This choice isolates the attenuation and sloping bottom effects from the water sound speed profile effect. For water depths less than the deep water depth of 1825 m, the SVP was truncated as the bathymetry varies. For example, only the first 430 m

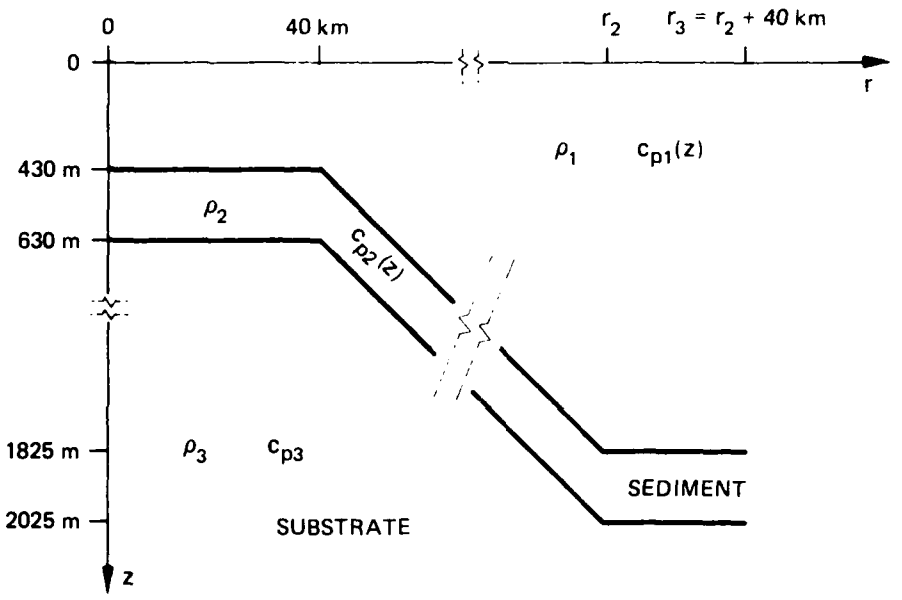

FIGURE 1
DOWNSLOPE GEOMETRY

ARL:UT
AS-82-165
RAK - GA
3 - 5 - 82

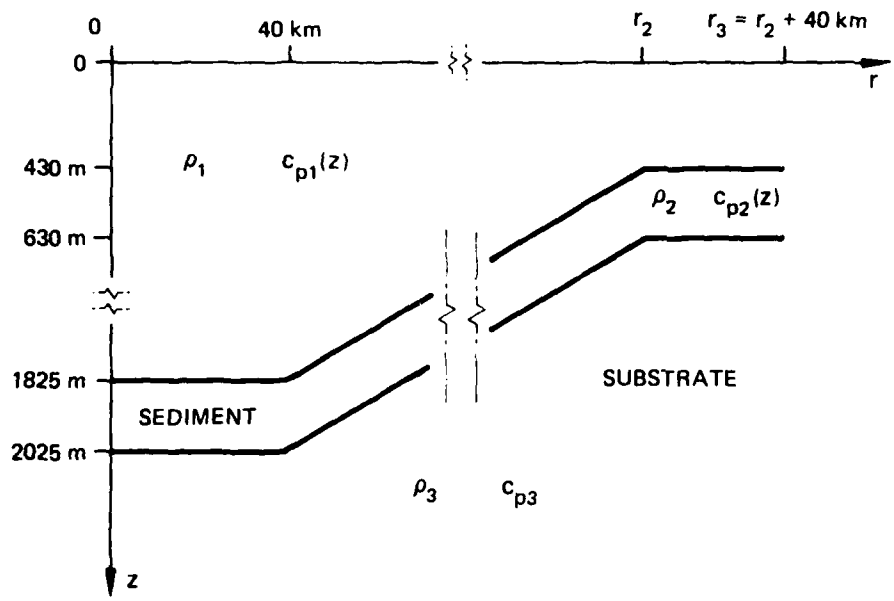

FIGURE 2
UPSLOPE GEOMETRY

ARL:UT
AS-82-166
RAK - GA
3 - 5 - 82

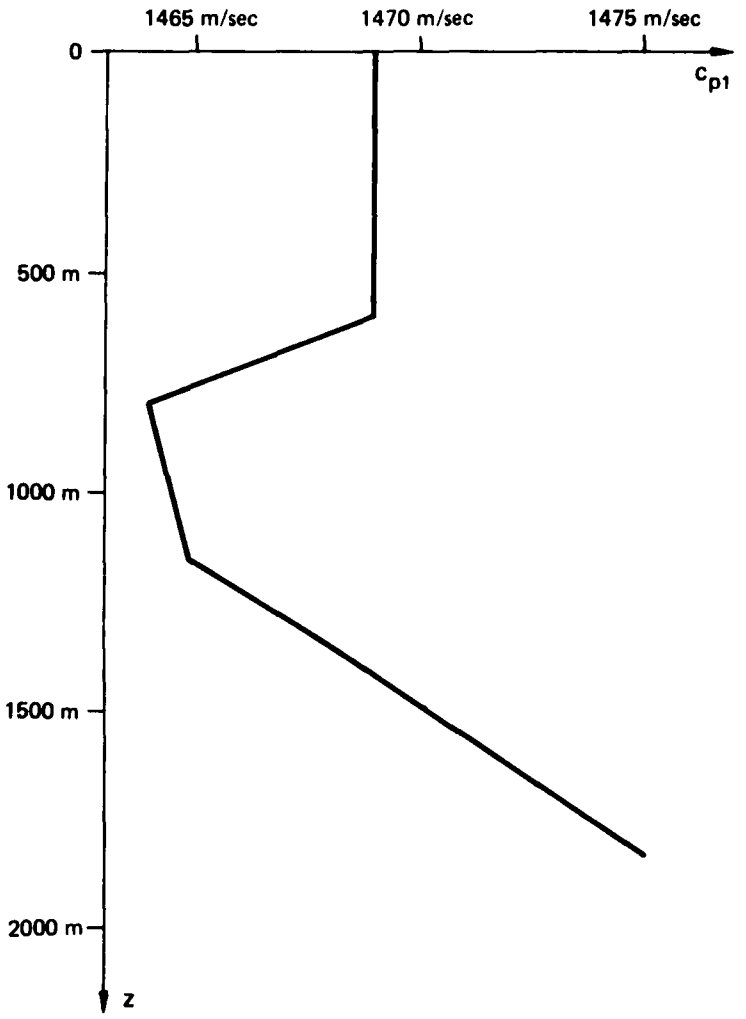

FIGURE 3
WATER SOUND VELOCITY PROFILE

ARL:UT
AS-82-167
RAK - GA
3 - 5 - 82

of the profile is used, where the water is shallowest. The water density used was 1.053 g/cm^3.

This study considers propagation over sloping bottom regions of three sediment types: clay, silt, and sand. The sediment layer is 200 m thick throughout the region r=0 to $r=r_3$. The density and surficial sound speed used for each sediment type are given in Table I. The sound speed gradient used is 1.0 (m/sec)/m for all sediment types. The values were chosen to be representative of those given by Hamilton[11] to the extent that density and sound speed for each sediment type are in the range of the quoted average values. However, the ratio of surficial sediment sound speed to water sound speed is not kept constant along the slope, as was done in the FY 80 study,[9] with no qualitative changes. More comment concerning velocity contrasts appears in Section II.B.2. All sediment types are assumed to be fluids.

The substrate is assumed to be a homogeneous half-space as specified in Table I. The substrate is assumed to be a fluid, whereas in 1980[9] the substrate was assumed to be a solid. Again, a comparison of the results with this work shows no qualitative changes. This change was made to simplify the normal mode computations and to acknowledge the fact that the importance of sediment (and substrate) rigidity is a function of such properties as sediment thickness and water depth. A compressional speed of 2700 m/sec has been chosen for the substrate although a speed of 5000 m/sec is more appropriate for basalt because the 200 m thick sediment strongly attenuates those higher order modes which interact with the substrate. The use of 2700 m/sec, which is a typical shear velocity for basalt, rather than 5000 m/sec for the substrate compressional speed serves to remove only these higher order modes from the calculation. These higher order modes would also be removed from the calculation if a solid description of the basalt were used. Consideration of such factors as thinner sediments and bottom rigidity on propagation in range variable environments is deferred to future work.

TABLE I

SEDIMENT AND SUBSTRATE GEOACOUSTIC PARAMETERS

Type	Density (g/cm^3)	Compressional Speed At Top of Layer (m/sec)
Clay	1.25	1525
Silt	1.6	1560
Sand	2.1	1725
Substrate	2.7	2700

In this study only sediment attenuation is allowed to vary. The water attenuation is neglected for the low frequency (100 Hz) considered here. The substrate attenuation is fixed to be 0.2 dB/m/kHz. The three sediment attenuation values employed in the study--0.0, 0.025, and 0.007 dB/m/kHz--are from a range of values appropriate for a high porosity sediment. (For sand these values are unrealistically low, but our conclusions are unchanged because they do not depend on particular parameter values but are based upon the important mechanisms. This point will be verified in Section II.B.2.)

For the cases presented here, eight different mode sets were used to represent the adiabatic variation of modes from deep to shallow water or vice versa. Each mode set is identified with the midpoint of a range interval or bin (except the first and last mode sets, which are identified with source and receiver ranges).

B. Downslope Propagation

1. Basic Mechanisms

As discussed in Ref. 9, the basic mechanisms involved in downslope propagation are spreading loss, shallow water attenuation, renormalization loss, and mode effectiveness. The relative importance of these mechanisms for the parameter values of interest determines the sensitivity of propagation, as measured by propagation loss, for example, to changes of those parameters. For an environment with no azimuthal dependence, the spreading loss contribution to propagation loss is independent of everything except range from source to receiver. Thus the magnitude of spreading loss may be used as a measure of the importance of the other mechanisms and of the sensitivity of propagation to parameter variations. On the other hand, renormalization loss is dependent upon the change, between source and receiver, in the effective vertical extent of the sound channel. This effective vertical extent,

H_{eff}, does depend upon the form of the SVP, bottom geoacoustic profile, and mode number. Thus, the importance of renormalization loss may be dependent upon sediment type and the combination of source depth and receiver depth. For the mechanism of attenuation and mode effectiveness, the analysis is not so simple because their effect on acoustic transfer between source and receiver depends upon the waveguide properties at intermediate ranges.

2. Sediment Type Effects

The downslope propagation results are illustrated in Figs. 4-7. These figures show the incoherent propagation loss as a function of range for the three sediment types and for different attenuation coefficient values. To simplify the display, the 0 dB/m/kHz results corresponding to the three sediments were combined into one reference curve which differs by less than 1 dB from the displayed curve. Figures 4-7 differ in the combination of source depth and receiver depth. The arrows above the range axis show the beginning and end of the sloping bottom region.

The steplike behavior of the incoherent propagation loss curves in Figs. 4-7 and others to follow reflects the discretization of the range variation as implemented in the adiabatic normal mode model.[9] Smoothing of the incoherent propagation loss versus range by the windowed range average employed in Ref. 9 was not used because the jumps in these curves give information concerning the action of propagation mechanisms (when analysis using this information is discussed, more details will be supplied). In the downslope propagation cases the steplike behavior occurs, if at all, at the crossing from one range bin to the next. At these crossings the adiabatic model begins calculations with the eigenmode set for the new range bin, i.e., no interpolation is used for the eigenfunctions between ranges associated with the environmental information used to calculate the eigenmode sets. On the other hand, the phase integrals describing the rapid range dependence of

In this study only sediment attenuation is allowed to vary. The water attenuation is neglected for the low frequency (100 Hz) considered here. The substrate attenuation is fixed to be 0.2 dB/m/kHz. The three sediment attenuation values employed in the study--0.0, 0.025, and 0.007 dB/m/kHz--are from a range of values appropriate for a high porosity sediment. (For sand these values are unrealistically low, but our conclusions are unchanged because they do not depend on particular parameter values but are based upon the important mechanisms. This point will be verified in Section II.B.2.)

For the cases presented here, eight different mode sets were used to represent the adiabatic variation of modes from deep to shallow water or vice versa. Each mode set is identified with the midpoint of a range interval or bin (except the first and last mode sets, which are identified with source and receiver ranges).

B. Downslope Propagation

1. Basic Mechanisms

As discussed in Ref. 9, the basic mechanisms involved in downslope propagation are spreading loss, shallow water attenuation, renormalization loss, and mode effectiveness. The relative importance of these mechanisms for the parameter values of interest determines the sensitivity of propagation, as measured by propagation loss, for example, to changes of those parameters. For an environment with no azimuthal dependence, the spreading loss contribution to propagation loss is independent of everything except range from source to receiver. Thus the magnitude of spreading loss may be used as a measure of the importance of the other mechanisms and of the sensitivity of propagation to parameter variations. On the other hand, renormalization loss is dependent upon the change, between source and receiver, in the effective vertical extent of the sound channel. This effective vertical extent,

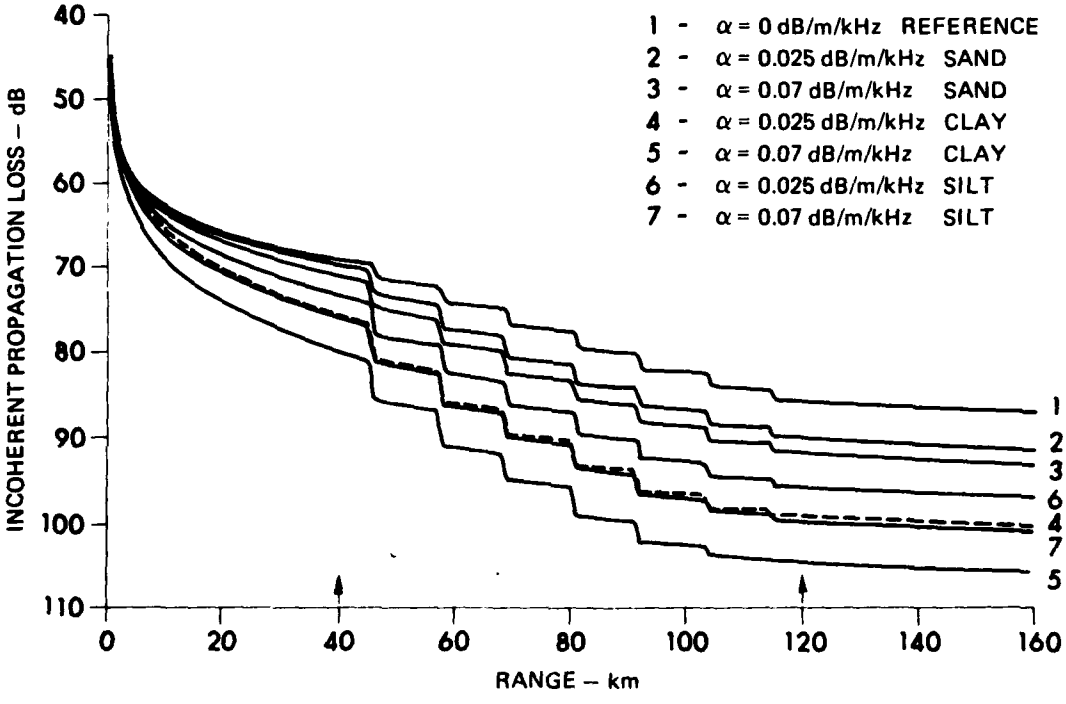

FIGURE 4
DOWNSLOPE PROPAGATION LOSS versus RANGE AND SEDIMENT ATTENUATION FOR CLAY, SILT, AND SAND
SOURCE DEPTH: 18 m RECEIVER DEPTH: 18 m
BOTTOM SLOPE: 1°

ARL:UT
AS-82-168
RAK - GA
3 - 5 - 82

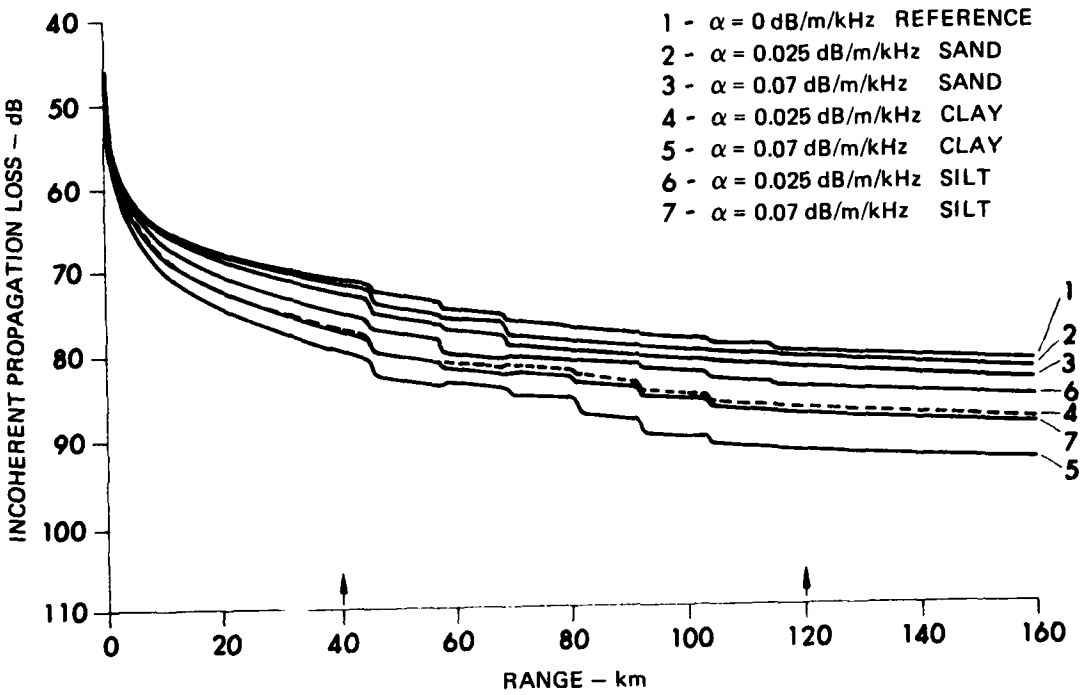

FIGURE 5
DOWNSLOPE PROPAGATION LOSS versus RANGE AND SEDIMENT ATTENUATION FOR CLAY, SILT, AND SAND
SOURCE DEPTH: 18 m RECEIVER DEPTH: 91 m
BOTTOM SLOPE: 1°

ARL:UT
AS-82-169
RAK - GA3
3 - 5 - 82

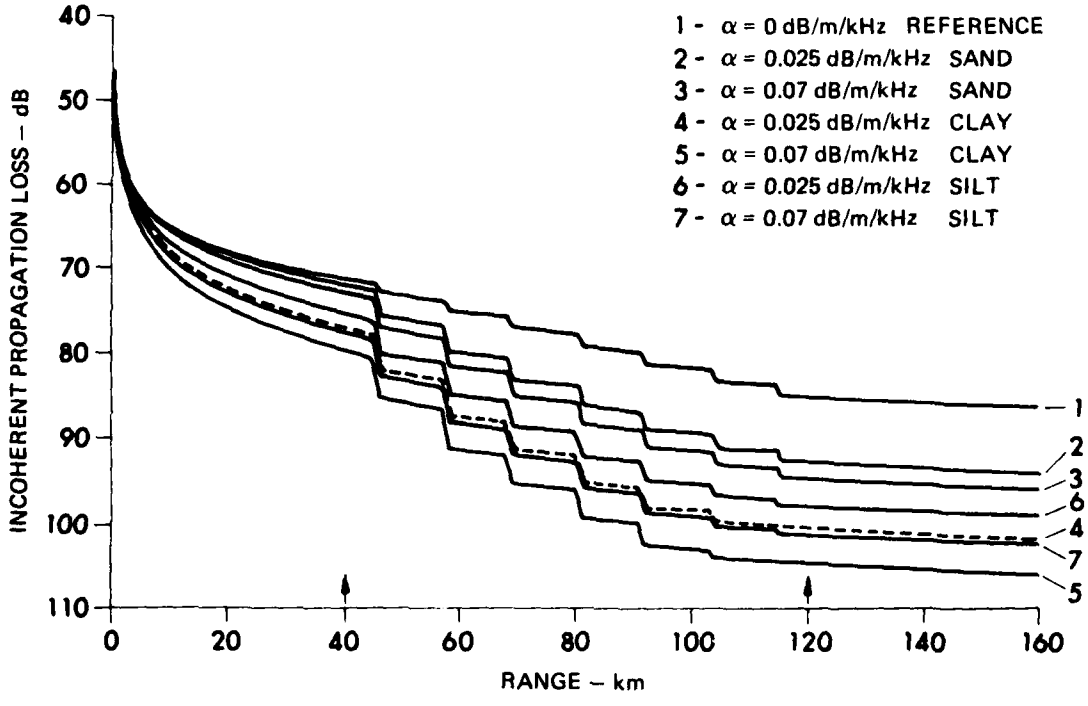

FIGURE 6
DOWNSLOPE PROPAGATION LOSS versus RANGE AND SEDIMENT ATTENUATION FOR CLAY, SILT, AND SAND
SOURCE DEPTH: 91 m RECEIVER DEPTH: 18 m
BOTTOM SLOPE: 1°

ARL:UT
AS-82-170
RAK - GA
3 - 5 - 82

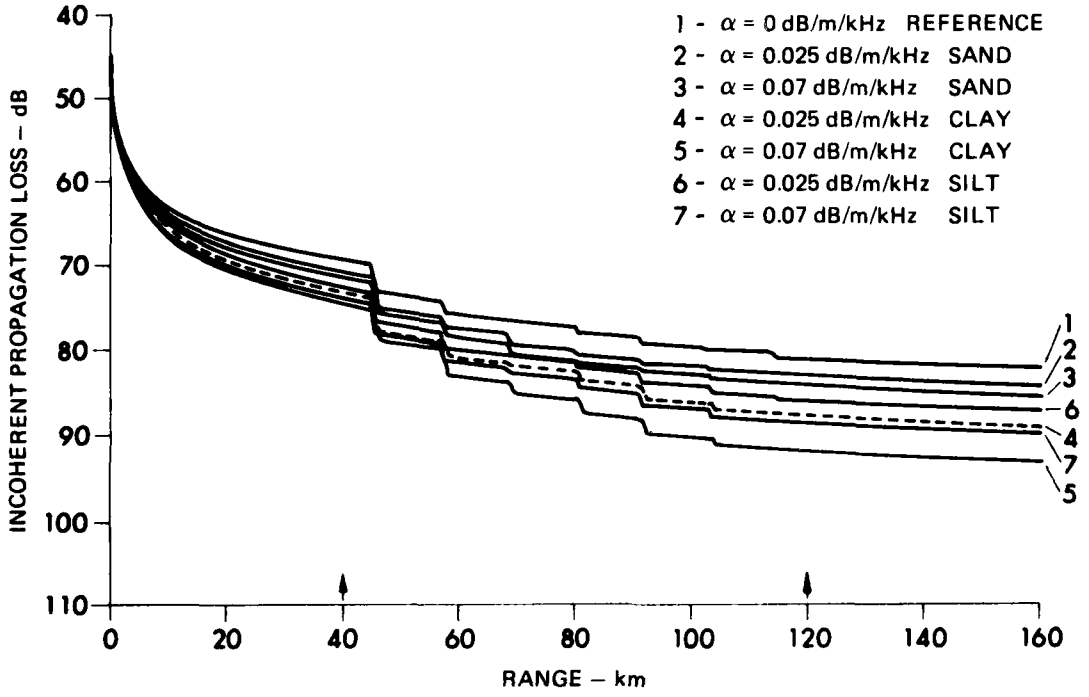

FIGURE 7
DOWNSLOPE PROPAGATION LOSS versus RANGE AND SEDIMENT ATTENUATION FOR CLAY, SILT, AND SAND
SOURCE DEPTH: 91 m RECEIVER DEPTH: 91 m
BOTTOM SLOPE: 1°

ARL:UT
AS-82-171
RAK - GA
3 - 5 - 82

the acoustic field do not contain abrupt changes in the adiabatic model because splines are used to fit the eigenvalue range dependence. The phase integral information is important in determining convergence zones or any interference phenomena. An accurate representation of the phase integrals across range bin boundaries is more important than an accurate interpolation of the eigenfunction. The phase integral error cumulates whereas the errors in eigenfunction are typically largest near the range bin boundaries but vanish at the ranges corresponding to the eigenmode sets. In the limit that the range bin width goes to zero, the exact adiabatic result is obtained. In many cases, a relatively coarse sampling (large range bins) is adequate.

In the discussion to follow, the sensitivity of results to parameter variations, particularly sediment attenuation, is considered. Qualitatively, a result is sensitive to parameter variations if small absolute changes in parameter values produce large absolute changes in the result; it is this sense that is meant in the present discussion. In applications a more quantitative specification is required. For example, if propagation loss must be known within 3 dB, then how accurately must sediment attenuation be known? (This quantitative sense appears in Section V.)

Each of the Figs. 4-7 shows that the sensitivity of propagation loss to the value of sediment attenuation decreases with increasing acoustic impedance contrast (clay to silt to sand) at the water-sediment interface. This result agrees with the notion that the smaller the impedance contrast, i.e., the softer the sediment, the more the acoustic field penetrates the sediment and interacts with an attenuating medium.

Each of the Figs. 4-7 shows also that sensitivity to sediment attenuation increases as the receiver location traverses the slope toward deeper water. The 1980 report[9] notes this result and ascribes it to the change in mode effectiveness between deep and shallow water. Briefly, the first mode dominates at all depths in the shallow water

because it is least attenuated. (The lowest order modes, which have the smallest phase velocities, are concentrated in the water column, i.e., regions with the smallest sound speed. As the mode number and phase velocity increase, the corresponding mode eigenfunctions extend into higher sound speed regions, e.g., the bottom.) In the deep water regions near the surface or bottom the first mode no longer dominates, i.e., only higher order modes couple well to a receiver near the surface or bottom, but in the shallow water regions these modes are most attenuated. Thus, as may be verified by comparing Figs. 4-7, the sensitivity of downslope propagation to attenuation depends not on the source depth (in shallow water), but on the receiver depth (in deep water). This conclusion would be modified if there were a sound channel in the shallow water region or if there were no sound channel in the deep water; however, understanding the mode effectiveness mechanism allows one to modify the conclusions without further modeling. For example, if a shallow water sound channel is present and the frequency is sufficiently high that one or more modes are effectively confined to the channel, then sensitivity to attenuation would also depend on the shallow water acoustic element depth. The presence of a significant sound channel means that sources off the channel axis will excite higher order modes more strongly than near-axis sources. Thus, the near-surface and near-bottom deep water acoustic field will depend upon shallow water source depth.

Another way of analyzing Figs. 4-7 is to note the difference in the sharp increases of propagation loss (artifacts of the environmental discretization) where the range bin boundary crossings occur, i.e., where there is a change in the eigenmode set used. These jumps are typically largest at the first bin crossing around a range of 42 km, for the largest value of attenuation, and for the shallower receiver depth. For example, Fig. 4 shows that for clay with an attenuation of 0.07 dB/m/kHz, at the first range bin crossing around 42 km there is a jump in propagation loss of approximately 4 dB. Of this value about 1.5 dB is attributable to renormalization loss due to a change in water depth from 430 m to 630 m. (The reference curve, for

zero sediment attenuation, shows approximately this change.) The remaining contribution to the 4 dB jump is associated with the downward shift, relative to the water surface, of the least attenuated low order modes and with the lack of compensating near-surface energy from the more heavily attenuated higher order modes. It is possible for the shifting of certain modes or groups of modes to produce the opposite effect over short range intervals, i.e., as the modes move in depth, an eigenfunction's amplitude at a given receiver depth can increase as a nearby null point in the eigenfunction moves farther down. This phenomenon occurred between 55 km and 60 km for the 18 m/91 m source depth/receiver depth combination results shown in Fig. 5. In this interplay between attenuation and effective mode mechanisms, sediment type mainly determines the amount of attenuation suffered by a mode, although it has some small effect in the details of the vertical shift of modes in the water column.

To verify that for sandy sediments the sensitivity of propagation to sediment attenuation does not increase at larger, more realistic values of attenuation, Fig. 8 shows the propagation loss over sand for attenuation values of 0.3 and 0.4 dB/m/kHz along with the results for the three lower values used earlier. The source and receiver are both at a depth of 18 m. In this more realistic range of attenuation values incoherent propagation loss is less sensitive to the precise value of attenuation than it is at lower values of attenuation appropriate for softer sediments (see Fig. 4). A change of 0.05 dB/m/kHz in sediment attenuation produces a change of about 5.5 dB in propagation loss for clay (Fig. 4), whereas twice that change in sediment attenuation produces 2.8 dB change in propagation loss over sand (Fig. 8). The reason for this decrease in sensitivity is that as sediment attenuation values increase the highest order modes are practically eliminated at longer ranges. At long ranges with increasing sediment attenuation value, only the lower order modes remain. Their levels are relatively independent of the sediment attenuation value, compared to the effect on higher order modes, because the lower order modes interact most weakly with the bottom, especially when it is hard.

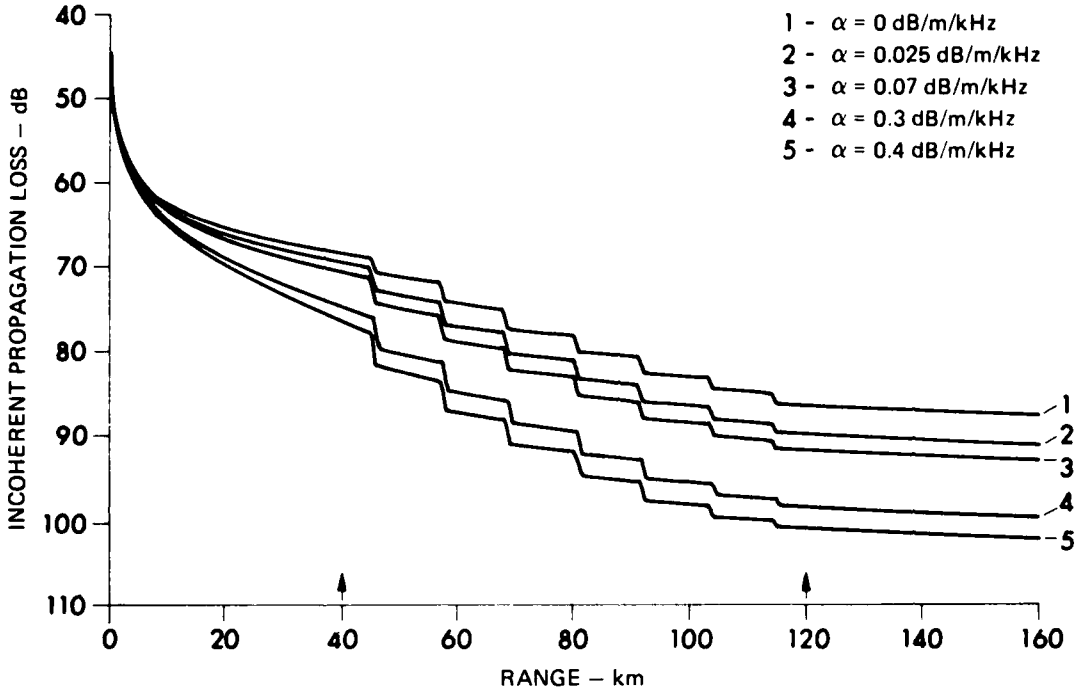

FIGURE 8
DOWNSLOPE PROPAGATION LOSS versus RANGE AND SEDIMENT ATTENUATION FOR SAND
SOURCE DEPTH: 18 m RECEIVER DEPTH: 18 m
BOTTOM SLOPE: 1°

ARL:UT
AS-82-172
RAK - GA
3 - 5 - 82

Figure 8 also shows quite clearly the increased importance of the effective mode mechanism as attenuation increases. Observe the jumps in propagation loss (artifacts of the chosen range discretization) just past 40 km, and note that the jump increases as attenuation increases. The explanation for this is that as attenuation increases, the higher order modes decrease more strongly in amplitude in the first 40 km. When the water depth increases, the maxima in the lower order mode amplitudes occur farther below the water surface. The decrease in the near-surface acoustic field is more noticeable, and the corresponding jump in propagation loss is larger, when the higher order modes are weaker due to stronger absorption in the sediment (larger values of attenuation). At the smaller values of sediment attenuation the higher order modes have larger amplitudes and their fields near the surface mask the decrease in the surface acoustic field due to decreases in the lower order mode amplitude near the surface.

Figures 4-7 show that sensitivity to sediment attenuation depends on sediment type. Whether this dependence on sediment type is actually dependence on impedance contrast rather than density contrast or velocity contrast, etc., was not directly examined in this study. However, some conclusions can be drawn from this work through comparisons with Ref. 9. In comparison with Ref. 9 where just a density contrast is used, the results obtained here have essentially the same curves for zero sediment attenuation, but the results of Ref. 9 show larger propagation losses for the same nonzero values of sediment attenuation. Upon noting that the density used in Ref. 9 was 1.4 g/cm^3, which is intermediate to the clay and silt densities used here, we suggest that the sensitivity of propagation to the attenuation values of soft sediments in shallow water is more dependent on the water-sediment sound speed ratio than on the density ratio.

3. Slope Angle Effects

For downslope propagation the effect of slope angle can be obtained from the results of Figs. 4-7 by a simple procedure. First,

the range axis in the sloping region is rescaled so that the 1^{o} slope interval between 40 km and 120 km instead covers the range 40-67 km. The range invariant region between 0 km and 40 km is left unchanged, and the region from 120 km to 160 km instead becomes 67-107 km. Second, the propagation loss curves for ranges larger than 40 km are adjusted upwards by adding a range dependent term 10 log[r(km)/40 km], which removes the difference in spreading loss between the 1^{o} slope and the shorter 3^{o} slope. This procedure yields results that are consistent with the lack of dependence on slope angle as seen in the downslope results cited in Ref. 9. Aside from the rescaling, the effect of sediment type and the interplay between the propagation mechanisms is identical to that given for the 1^{o} results. Further discussion of slope angle independence and the presentation of model results are deferred to Section II.C.3.

4. Energy Partitioning

An examination of the distribution of power between waterborne and bottom interacting modes is useful in determining ranges at which bottom interaction is important and at which shifts between waterborne and bottom interacting energy take place. A particular mode at some receiver range may be classified as waterborne or bottom interacting depending on whether the horizontal phase speed is less than or greater than, respectively, the water sound speed at the sediment surface. This corresponds to the condition that a mode turning point cross from the water into the sediment or, in the ray approximation, a ray penetrate into the sediment.

The power radiated into a given mode is determined by the coupling between that mode and the source. The power is carried by the mode as a whole and is not associated with any particular depth. The coupling between a mode and the source, and hence the radiated power, does depend upon the value of the mode at the source depth. Thus the power in a particular mode depends on the source depth and is independent of receiver depth.

Figures 9 and 10 show the waterborne and bottom interacting power, respectively, as a function of range for the case of propagation down a 1^{0} slope. The source depth is 18 m. In Fig. 9 the waterborne power does not appear until around 80 km where the sound channel becomes part of the SVP. On the other hand, Fig. 10 shows that the bottom interacting power is essentially constant over the range 40-90 km, i.e., between the shallow end of the slope and the point where bottom interacting modes change over into waterborne modes. Again, the conclusion is that the sensitivity to attenuation observed in the propagation loss occurs in the shallow water environment, i.e., the power dissipated due to absorption in the sediment is determined primarily by the shallow water sediment attenuation value rather than the sediment attenuation values on the slope or in deep water.

The waterborne and bottom interacting power versus range for a source depth of 91 m were examined but are not shown here. For this deeper source, the case when the sediment attenuation is nonzero has more waterborne and less bottom interacting power in the sound field in deep water compared to the levels in Fig. 9. This source depth dependence does account for the small differences between Figs. 4 and 6 or between Figs. 5 and 7. The larger differences between Figs. 4 and 5 or between Figs. 6 and 7 occur because the coupling to a receiver by a given mode is strongly dependent on depth in a depth dependent sound speed profile, whereas source excitation of a given mode is weakly dependent on depth in isovelocity water.

5. Depth Dependence

As the sound field from a source in shallow water propagates to deeper water, the depth dependence of the field is affected by several environmental parameters. These parameters control the relative importance of the attenuation and mode effectiveness mechanisms.

A convenient concept embodying the key features of the mutual interaction of attenuation and mode effectiveness can be further

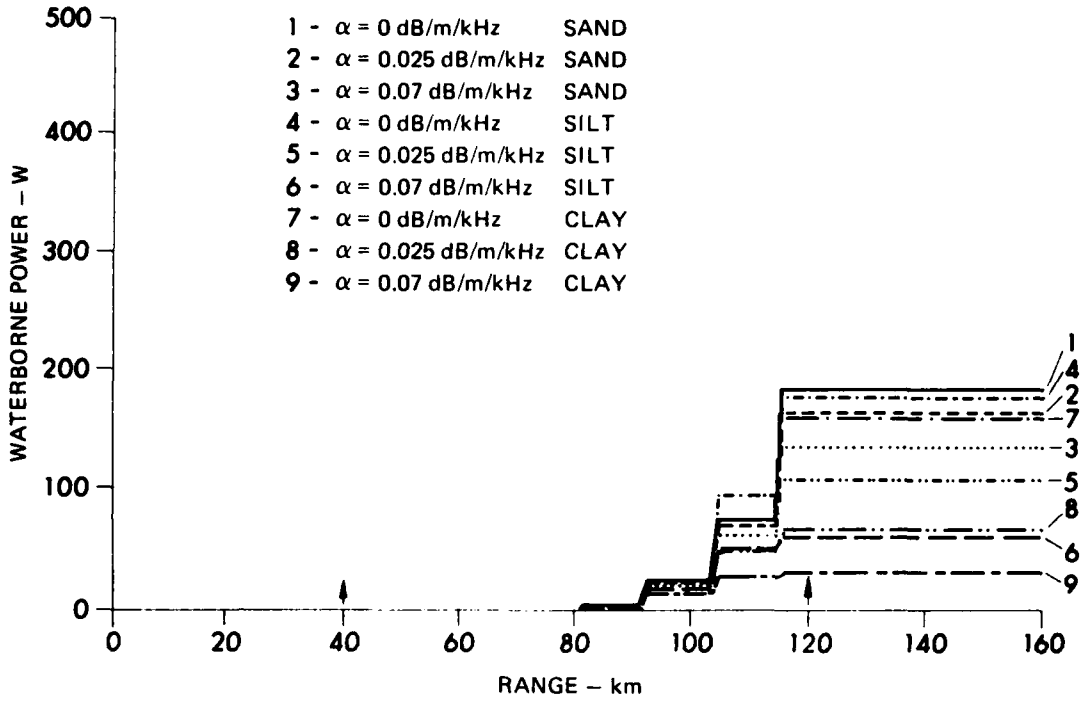

FIGURE 9
POWER IN WATERBORNE MODES versus RANGE AND SEDIMENT ATTENUATION FOR CLAY, SILT, AND SAND
SOURCE DEPTH: 18 m
BOTTOM SLOPE: 1° DOWN

ARL:UT
AS-82-173
RAK - GA
3 - 5 - 82

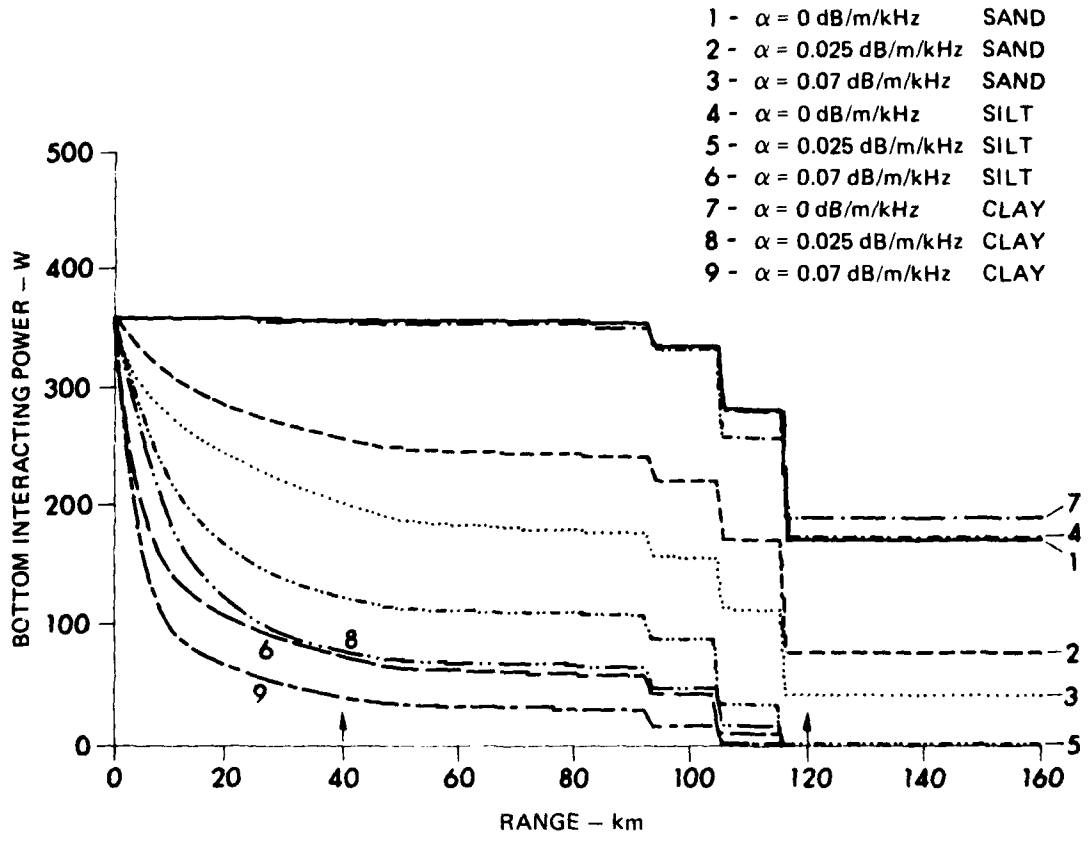

FIGURE 10
POWER IN BOTTOM INTERACTING MODES versus RANGE AND SEDIMENT ATTENUATION FOR CLAY, SILT, AND SAND
SOURCE DEPTH: 18 m
BOTTOM SLOPE: 1° DOWN

ARL:UT
AS-82-174
RAK-GA
3-5-82

developed from the discussion of renormalization in Section II.B.1. Let H_{eff} be the effective extent of the waveguide in depth for a given mode, i.e., the depths occupied by the mode. H_{eff} is a function of mode number and range, because the portion of the water column or sediment occupied by a given mode depends on range through the SVP and the water depth. If the vertical extent defined by H_{eff} at a given range includes the bottom, then sediment attenuation will be an active mechanism at that range for that mode; this is typical for shallow water. For deep water with a sound channel it is possible that the lower modes will have H_{eff} entirely within the water column; for these modes attenuation is not an important mechanism at that range. In either deep or shallow water H_{eff} is typically smaller for the lower order modes. Higher order modes, which are more bottom interacting, become less important with increasing range provided that both the source and receiver couple well to the lower order modes. This will occur when the waveguide sections, defined by H_{eff} for the lower order modes, overlap along the propagation path to a high degree and contain the source and receiver depths at either end. Thus the effectiveness of a particular mode in propagation between some particular source and receiver depends upon the overlap of H_{eff} with (1) the source, which governs the energy coupled into the mode, (2) the receiver, which governs the energy coupled out of the mode, and (3) the bottom along the propagation path, which governs the attenuation of the mode.

One conclusion to be drawn from these observations is that H_{eff} of the effective modes will determine the depth dependence of the deep water sound field produced by sources in shallow isovelocity water. The effective modes are the modes which were excited by the source and were relatively unattenuated over the propagation path. If there remain only a few lower modes whose H_{eff} is confined to the sound channel axis in deep water, the sound field will be concentrated near this axis. If higher order modes whose H_{eff} can extend far above and below the channel axis survive, the deep water sound field will be distributed more evenly over the water column. For sources in isovelocity shallow water where H_{eff} contains the entire water column for most of the modes, the source

depth is not particularly important in determining the depth dependence in deep water. In shallow water with a sound channel present the sources in the channel, as opposed to near-surface or near-bottom sources not in the channel, would produce a sound field much more concentrated around the deep water channel axis. In this case, for the lower order modes, H_{eff} is confined to the channel axis and does not include the bottom anywhere between source and receiver. For higher order modes H_{eff} includes the bottom everywhere between source and receiver, and these modes are strongly attenuated. Thus the sound field is concentrated in the channel everywhere between source and receiver.

Considerations of source and receiver depth dependence based upon the mechanism viewpoint were illustrated for a given sediment type in Ref. 9. Figure 11 demonstrates the receiver depth dependence for different sediments. Here the depth dependence of the sound field propagated down a 1^{o} slope from a source 18 m deep is given for a reference sediment with no sediment attenuation and for clay and sand sediments with 0.07 dB/m/kHz attenuation. The reference curve is actually for sand, but the corresponding curve for clay is basically identical. Note that the reference curve shows the sound field to be nearly uniformly distributed across the water column except very near the surface and very near the bottom. This is the result of a large number of effective modes having survived over the propagation path. The depth dependence for the clay sediment shows that the sound field is somewhat more confined to the interior of the water column. For the sand sediment, the sound field extends much closer to the bottom. This is a result of the reduced penetration of the sound field into the harder sand bottom leading to a reduction in the attenuation of the higher modes which contribute to the near-bottom field. However, for the higher and more realistic attenuation values for sand sediments discussed in connection with Fig. 8, the higher modes are stripped from the sound field by the larger attenuation, so that the sound field depth dependence is more similar to that given for clay in Fig. 11.

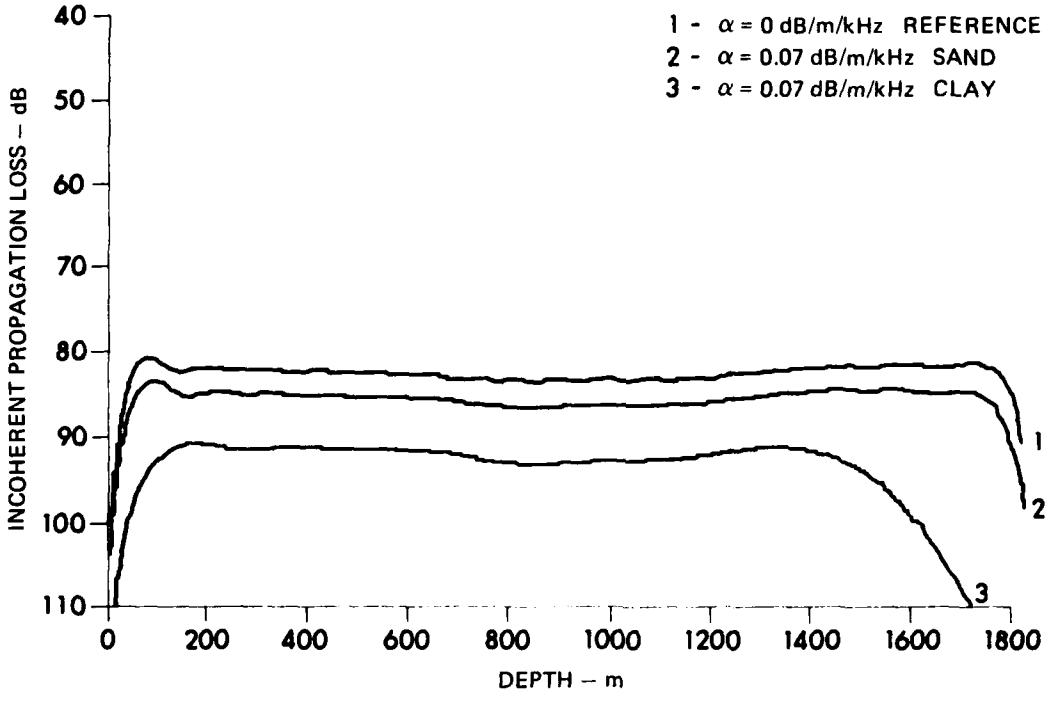

FIGURE 11
DOWNSLOPE PROPAGATION LOSS versus DEPTH AND SEDIMENT ATTENUATION FOR CLAY AND SAND
SOURCE DEPTH: 18 m RANGE: 160 km
BOTTOM SLOPE: 1°

ARL:UT
AS-82-175
RAK - GA
3 - 5 - 82

C. Upslope Propagation

1. Basic Mechanisms

The upslope mechanisms include the mechanisms of downslope propagation listed in Section II.B.1 and, in addition, the mechanism of mode cutoff as discussed in Ref. 9. Typically, as the water depth decreases, the modes with the largest mode number are no longer bound by the waveguide but radiate into the bottom. In this report attention will be directed primarily to the effect of sediment type on determining the relative importance of these mechanisms and the sensitivity of propagation to sediment attenuation.

2. Sediment Type Effects

Upslope propagation results are shown in Figs. 12-15. These figures show the incoherent propagation loss as a function of range for the three sediment types and for different attenuation values. To simplify the display the 0 dB/m/kHz results for each of the three sediments were combined into one reference curve which differs by less than 1 dB from the computed values. Figures 12-15 differ in the combination of source and receiver depth. The deep water end of the slope is at 40 km range, and the shallow water end is at 120 km range.

In Figs. 12-15 the discretization of the sloping bottom in the adiabatic propagation model gives rise to two types of artifacts. The first of these artifacts is a discontinuity in the incoherent propagation loss curves when the range bin boundaries are crossed. This artifact was discussed in detail in Section II.B.2 for downslope propagation. The second artifact occurs midway between the range bin crossings and is associated with mode cutoff in upslope propagation. Mode cutoff in the adiabatic approximation is the total loss by radiation into the bottom of whatever energy is in the highest order modes. The loss of modes through cutoff occurs because the number of modes which exist in a waveguide decreases as the effective depth of the

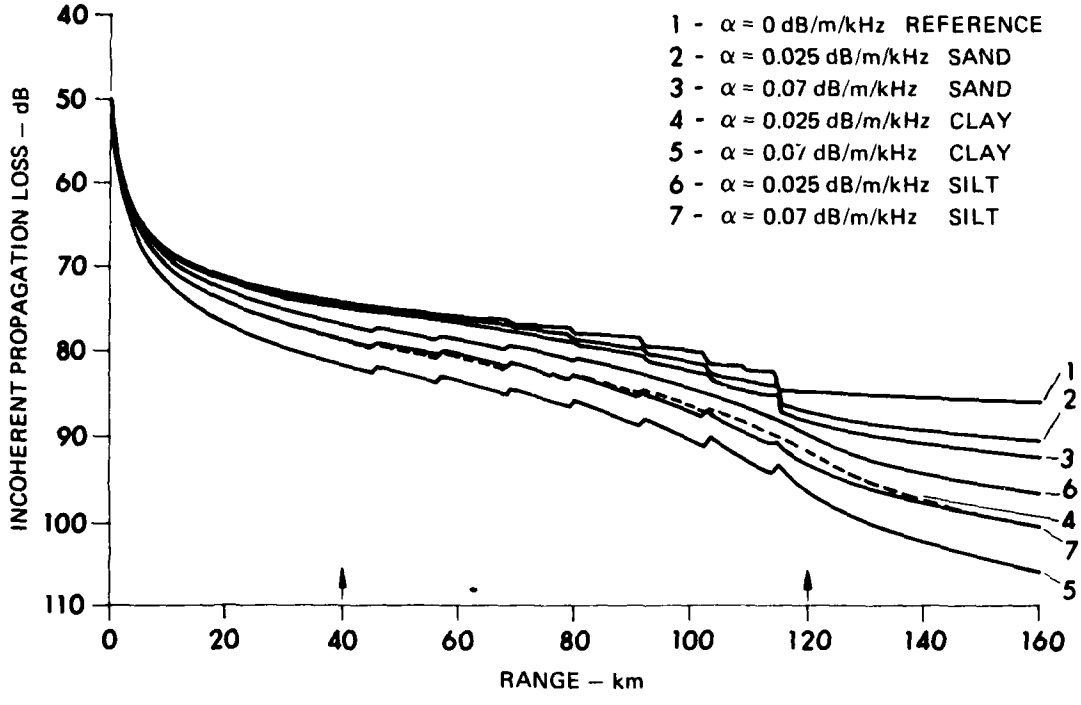

FIGURE 12
UPSLOPE PROPAGATION LOSS *versus* RANGE AND SEDIMENT ATTENUATION FOR CLAY, SILT, AND SAND
SOURCE DEPTH: 18 m RECEIVER DEPTH: 18 m
BOTTOM SLOPE: 1°

ARL:UT
AS-82-176
RAK - GA
3 - 5 - 82

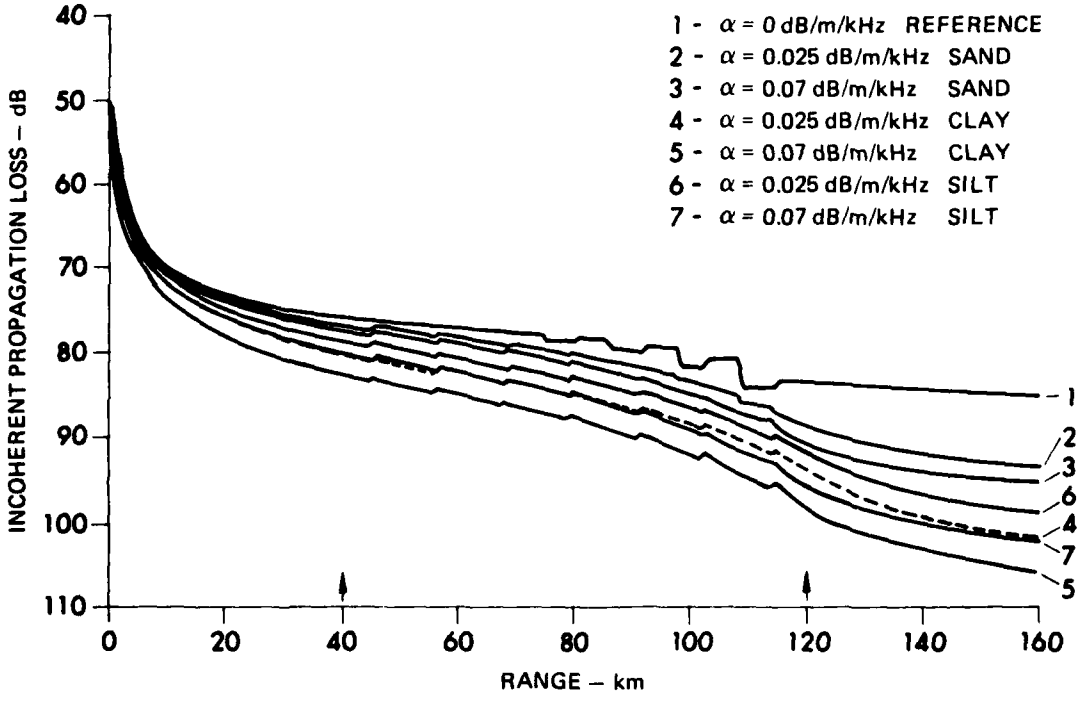

FIGURE 13
UPSLOPE PROPAGATION LOSS versus RANGE AND SEDIMENT ATTENUATION FOR CLAY, SILT, AND SAND
SOURCE DEPTH: 18 m RECEIVER DEPTH: 91 m
BOTTOM SLOPE: 1°

ARL:UT
AS-82-177
RAK - GA
3 - 5 - 82

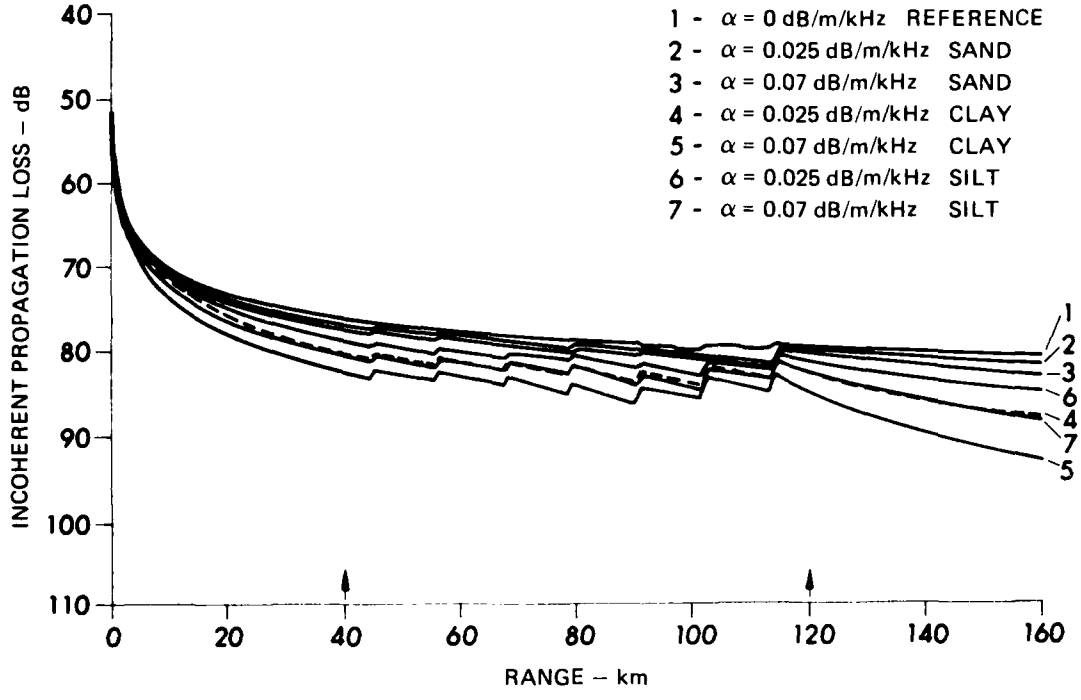

FIGURE 14
UPSLOPE PROPAGATION LOSS versus RANGE AND SEDIMENT ATTENUATION FOR CLAY, SILT, AND SAND
SOURCE DEPTH: 91 m RECEIVER DEPTH: 18 m
BOTTOM SLOPE: 1°

ARL:UT
AS-82-178
RAK - GA
3 - 5 - 82

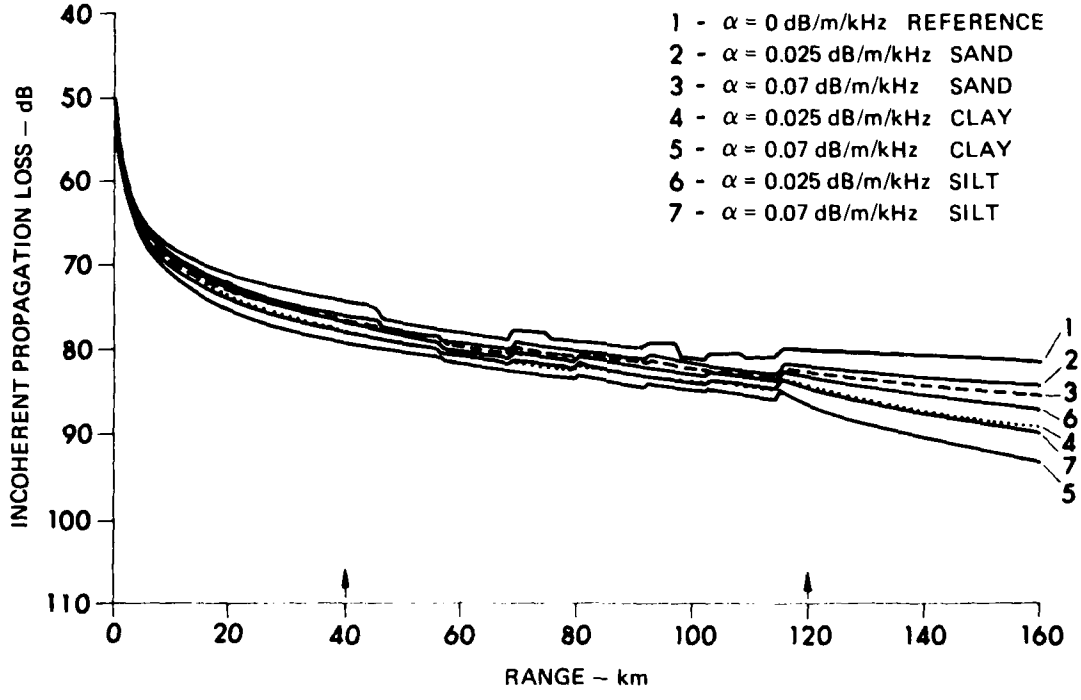

FIGURE 15
UPSLOPE PROPAGATION LOSS versus RANGE AND SEDIMENT ATTENUATION FOR CLAY, SILT, AND SAND
SOURCE DEPTH: 91 m RECEIVER DEPTH: 91 m
BOTTOM SLOPE: 1°

ARL.UT
AS-82-179
RAK - GA
3 - 5 - 82

waveguide decreases. Because the mode eigenvalues are not computed once a mode has gone past cutoff, information about the eigenvalue versus range is not available beyond the range associated with the last range bin containing that eigenvalue. Instead, these modes, having nearly reached cutoff, are dropped from the computations at the center of that range bin. These two processes are particularly evident in the reference curve in Fig. 13 over the ranges 80-120 km. The sudden increases in propagation loss associated with mode cutoff alternate with sudden decreases in propagation loss associated with renormalization gain and mode effectiveness. The renormalization gain is the decrease in propagation loss produced when the acoustic field is "compressed" as the effective depth of the waveguide decreases for sound propagating upslope. Note that a finer sample of the range variation would show a smoother behavior in propagation loss versus range, but would not change the net effect of the processes identified with artifacts produced by this coarser sample.

Over the region of the slope, 40-120 km, four mechanisms are particularly evident in the artifacts. These are: mode effectiveness, mode cutoff, renormalization, and attenuation. For the reference curves attenuation plays no role. The results of the competition between the other three mechanisms will depend upon both the source depth and the receiver depth. For the source and receiver combination in Figs. 12 and 13 the reference curve shows an overall increase in propagation loss, with all three processes most pronounced (both increases and decreases occur) in Fig. 13. These same effects nearly cancel in the reference curve of Figs. 14 and 15 (increases cancel decreases). However, for the largest attenuation values and softer sediments the attenuation effectively removes those modes which would be cut off. Renormalization and mode effectiveness remain to give the sudden decreases in propagation loss shown in curve 5 in Figs. 12-15. The portion of these jumps attributable to renormalization gain increases from 0.49 dB at the bottom of the slope to 1.7 dB at the top of the slope.

These results show that sediment type determines the sensitivity of propagation to attenuation. Again, the harder the sediment the more the sound field is confined to the water column and the less the sensitivity to the attenuation value assumed for the sediment. It is also clear from the behavior of the curves in Figs. 12-15 that past a range of 120 km the renormalization gain is quickly negated by attenuation in the shallow water, and the more so, the softer the sediment.

3. Slope Angle Effects

In the previous report[9] the results as presented give the impression of a strong dependence on slope angle for upslope propagation but not for the downslope case. This conclusion can be traced to the use of a longer range interval for the shallow water region following the 3^{o} slope than for the region following the 1^{o} slope. In this report this difference is removed, and the analysis and conclusions concerning the sensitivity of propagation to sediment attenuation as a function of slope angle will be seen to apply to both upslope and downslope propagation.

Figure 16 illustrates the case of propagation up a 3^{o} slope for source and receiver both at a depth of 18 m. The incoherent propagation loss is given as a function of source to receiver separation out to 107 km. Range invariant intervals 40 km in extent precede and follow the slope region as in Figs. 12-15. The zero attenuation curve is a reference similar to that used in Fig. 12. Just the results for silt and sand sediments with an attenuation value of 0.07 dB/m/kHz are given.

In Fig. 16 curve 3 especially demonstrates the "slope enhancement" effect. This effect is observed in some propagation loss measurements in which a fixed receiver in a deep water region monitors the acoustic field generated at source positions located at various points along a slope. The principle of reciprocity may be invoked to

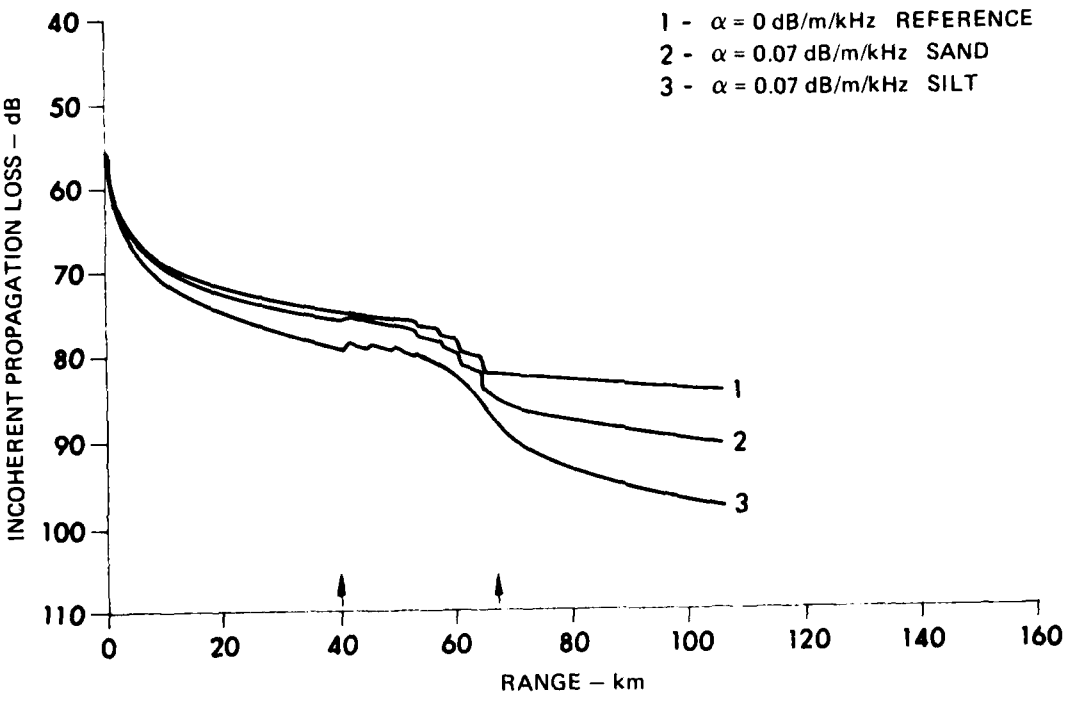

FIGURE 16
UPSLOPE PROPAGATION LOSS versus RANGE AND SEDIMENT ATTENUATION FOR SILT AND SAND
SOURCE DEPTH: 18 m RECEIVER DEPTH: 18 m
BOTTOM SLOPE: 3°

ARL:UT
AS-82-180
RAK-GA
3-5-82

interchange source and receiver positions so that the results in Fig. 16 apply. Thus, as the position of the moving acoustic element moves with increasing range in Fig. 16 up the slope from deep water to shallow water, the propagation loss decreases between 40 and 50 km before increasing again. As also holds for Figs. 12-15, this "slope enhancement" is a result of competition between loss due to cylindrical spreading, attenuation, and mode cutoff and gains due to renormalization and shifts in the effective modes for the given combination of source and receiver depths. At long ranges the spreading loss rate is small and attenuation tends to eliminate those modes which would otherwise be cut off. Considerations of slope enhancement can neglect both cutoff, when there are many modes, and spreading loss, at long ranges.

Comparison of Fig. 16 with the corresponding portions of Fig. 12 shows the curves to be quite similar except for a compressed range interval in Fig. 16 which emphasizes the gain by the renormalization effect relative to spreading loss and attenuation. In fact, a comparison of the numerical values for propagation loss at 160 km for the 1^{o} slope with the values at 107 km for the 3^{o} slope shows the former to be approximately 2 dB larger for each of the curves. This difference is mostly a result of the difference of 1.6 dB in spreading loss to be expected due to the difference in total range intervals. Some difference in propagation loss for the two slopes is also expected because of a difference in accumulated attenuation. Basically, for the same total depth change, a 1^{o} slope contains a longer range interval of higher attenuation, i.e., shallow water, than does a 3^{o} slope. Otherwise, within the adiabatic approximation, no dependence on slope angle can exist whether propagation is upslope or downslope. In particular, the effects of renormalization and the shift in depth of the effective modes are independent of slope angle. Thus, the "slope enhancement" effect depends on slope angle only through differences in accumulated attenuation and the actual range at which it occurs.

4. Energy Partitioning

Figure 17 shows the waterborne and bottom interacting power as a function of range for propagation up a 1^{o} slope from sources at depths of 18 m and 91 m. The sediment is sand with an attenuation of 0.07 dB/m/kHz.

For both of these source depths the bottom interacting modes dominate the propagation. A noticeable fraction of the power from the 91 m source is first in waterborne modes but is transferred into bottom interacting modes at the bottom of the slope between 40 km and 60 km. Thus, the upward jumps in curve 4 of Fig. 17 are associated with the drops in curve 2. Thereafter, the bottom interacting modes carry most of the power which is steadily reduced by attenuation. The upward jumps in curve 4 between 40 km and 60 km are power transfers from waterborne to bottom interacting modes and are not "slope enhancement" effects. The power in a mode, aside from attenuation losses, is a conserved quantity in the adiabatic approximation and is identified with the whole mode rather than a given depth. However, "slope enhancement" is partly associated with the change in power per unit depth which results from changes in water depth.

Figure 17 shows no sudden drops in the bottom interacting power. This indicates that the highest order modes, which are undergoing cutoff, carry a small fraction of the power at their cutoff range. The power from the shallower source (18 m) attenuates more rapidly than power from the deeper (91 m) source because the modes excited by a shallower source are higher order, hence more bottom interacting, than those excited by the deeper source.

5. Depth Dependence

The sound field dependence on source and receiver depths was discussed in some detail in Ref. 9. The conclusion there was that the shallow water field for upslope propagation depended most strongly on source depth, but was relatively insensitive to receiver depth. That

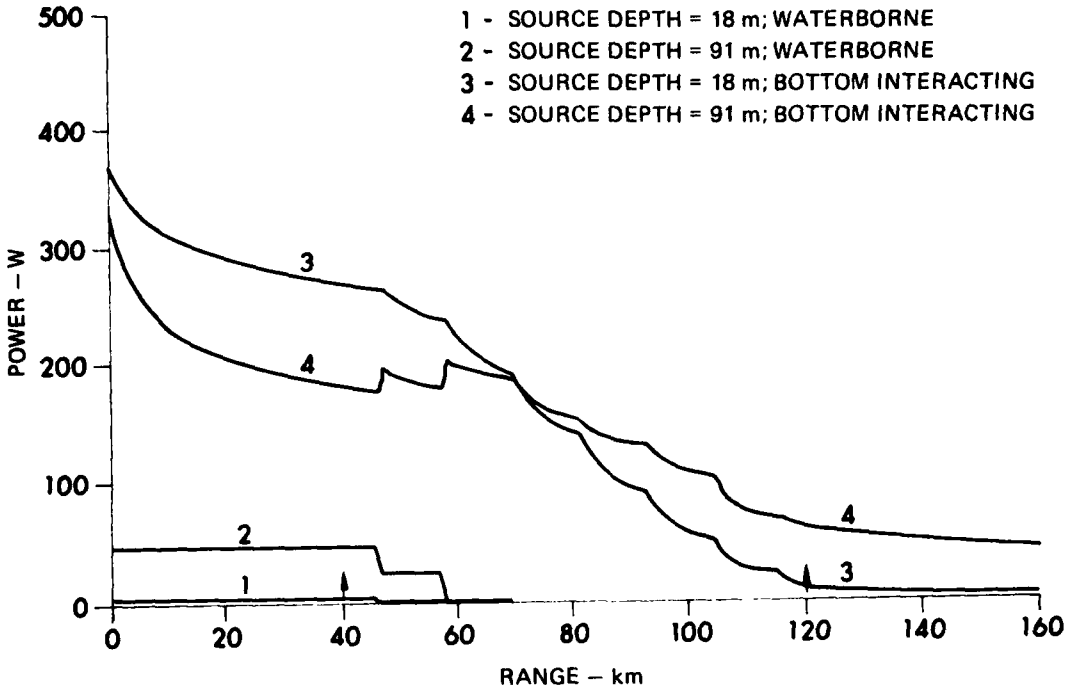

FIGURE 17
WATERBORNE AND BOTTOM INTERACTING POWER versus RANGE
BOTTOM SLOPE: 1° UP SEDIMENT TYPE: SAND
ATTENUATION: 0.07 dB/m/kHz

ARL:UT
AS-82-181
RAK - GA
3 - 5 - 82

conclusion is verified by the studies presented here. The dependencies of bottom interacting and waterborne power versus range for different source depths, as in Fig. 17, reflect this depth dependence.

6. Attenuation Gradient

For all of the model results presented thus far, the sediment attenuation has been taken as constant in depth. Figures 18-21 show the upslope propagation loss for several source-receiver configurations for a 200 m clay sediment layer with attenuation increasing linearly with depth from 0.025 dB/m/kHz at the sediment surface to 0.2 dB/m/kHz at the substrate. The resulting gradient, 8.75×10^{-4} dB/m^2/kHz is a compromise. This value is several times larger than might be expected for silt-clay but is of opposite sign and perhaps an order of magnitude less than expected for sand-silt, especially near the surface.[12] A problem with larger negative gradients is examined in Section III.C. For comparison each figure also shows the loss for two constant sediment attenuation values of 0.025 dB/m/kHz and 0.07 dB/m/kHz (see Figs. 12-15). Results for silt and sand sediments are qualitatively similar to those presented for clay, although propagation over the clay sediment was most sensitive to the presence of the attenuation gradient because the sound field penetrates farther into the softer sediment.

The most noticeable effect of the attenuation gradient occurs for the shallower source (Figs. 18 and 19) which excites more effectively the bottom interacting modes most sensitive to the gradient. The gradient affects propagation throughout the deep and sloping regions. However, as the sound field propagates farther into the shallow water region, the more strongly attenuated bottom interacting modes carry little energy, leaving only contributions from those modes which sample at most the top of the sediment layer. Thus the shallow water portion of the propagation loss curves, when there is a positive depth gradient of sediment attenuation, first approach the curves for a sediment with constant attenuation but with the same surface value. The same effect is also evident in the deep water portion of Figs. 18-21. From the

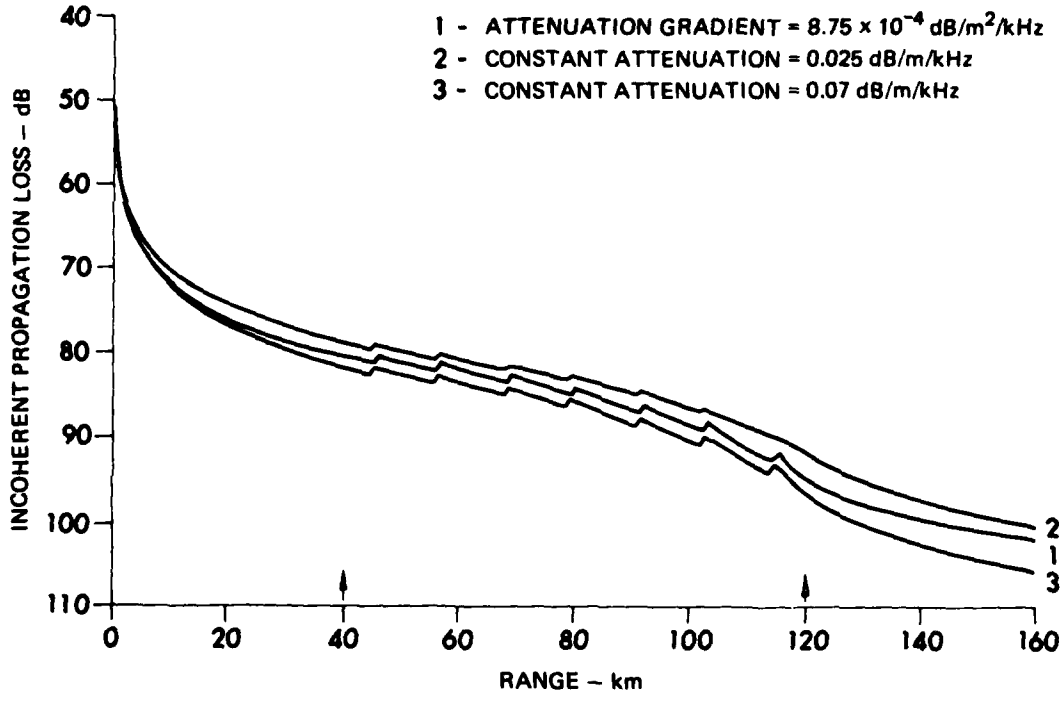

FIGURE 18
PROPAGATION LOSS versus RANGE WITH SEDIMENT ATTENUATION GRADIENT
SOURCE DEPTH: 18 m RECEIVER DEPTH: 18 m
SEDIMENT TYPE: CLAY BOTTOM SLOPE: 1° UP

ARL:UT
AS-82-182
RAK - GA
3 - 5 - 82

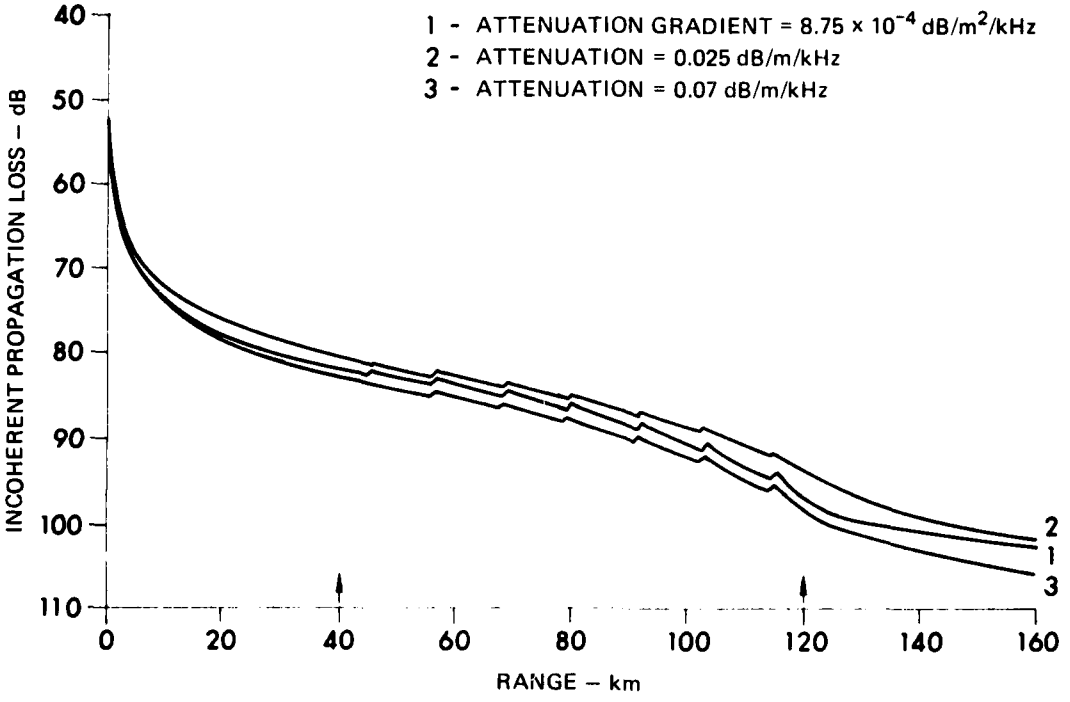

FIGURE 19
PROPAGATION LOSS versus RANGE WITH SEDIMENT ATTENUATION GRADIENT

SOURCE DEPTH: 18 m RECEIVER DEPTH: 91 m
SEDIMENT TYPE: CLAY BOTTOM SLOPE: 1° UP

ARL:UT
AS-82-183
RAK - GA
3 - 5 - 82

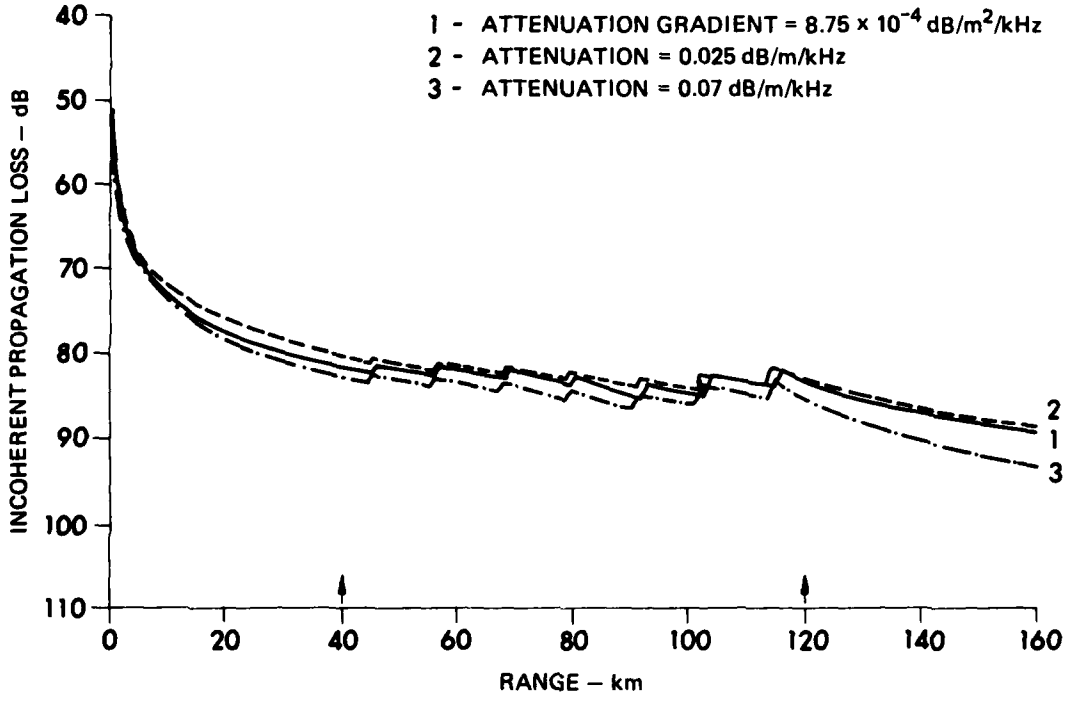

FIGURE 20
PROPAGATION LOSS versus RANGE WITH SEDIMENT ATTENUATION GRADIENT
SOURCE DEPTH: 91 m RECEIVER DEPTH: 18 m
SEDIMENT TYPE: CLAY BOTTOM SLOPE: 1° UP

ARL:UT
AS-82-184
RAK - GA
3 - 5 - 82

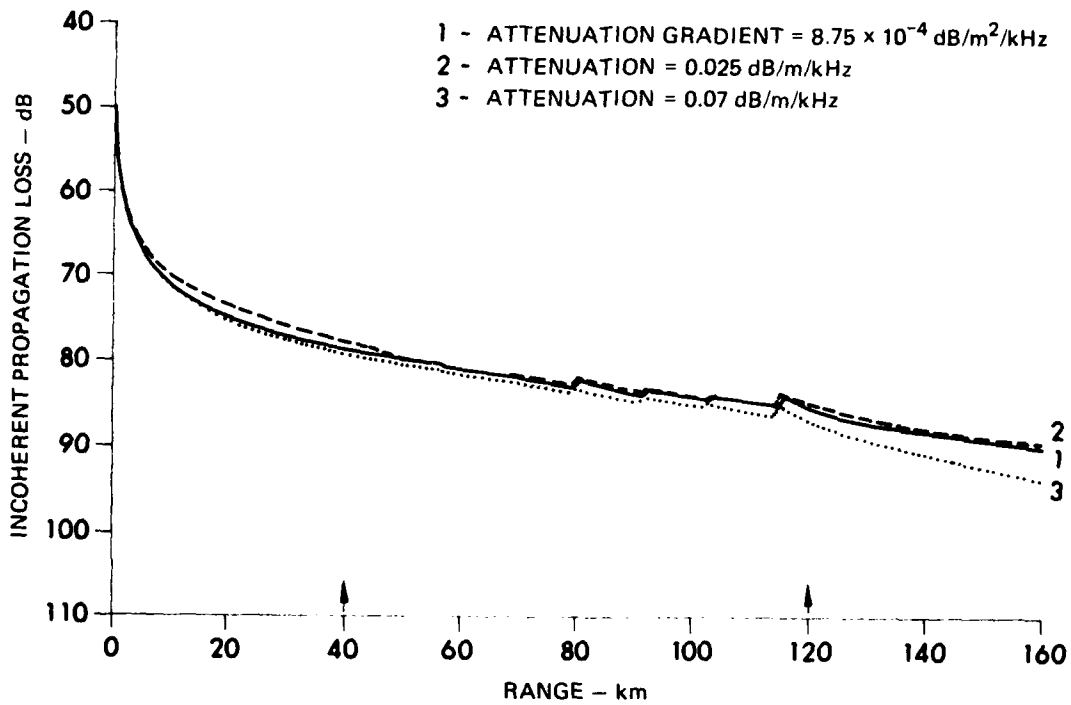

FIGURE 21
PROPAGATION LOSS versus RANGE WITH SEDIMENT ATTENUATION GRADIENT

SOURCE DEPTH: 91 m RECEIVER DEPTH: 91 m
SEDIMENT TYPE: CLAY BOTTOM SLOPE: 1° UP

ARL:UT
AS-82-185
RAK - GA
3 - 5 - 82

source, curve 1 in each figure diverges from curve 3 and approaches curve 2 until the slope is encountered at 40 km. After 120 km curve 1 continues to approach curve 2. On the slope, between 40 km and 120 km, curve 1 approaches curve 3 because the weakly bottom interacting modes penetrate more deeply into the sediment as the water depth decreases and thus sample the higher attenuation values resulting from the gradient. At longer ranges in shallow water curves 1 and 2 eventually diverge (see Fig. 21) because the attenuation coefficient of the most weakly attenuated (last remaining) mode must be larger for a positive attenuation gradient than without the gradient.

D. Conclusions

The mechanisms which determine the incoherent propagation loss over a sloping thick sediment bottom are spreading loss, renormalization, mode effectiveness, and attenuation within the sediment. These are active in either upslope or downslope propagation. An additional mechanism active in upslope propagation is mode cutoff. These mechanisms operate for all sediment types.

The sensitivity of propagation to sediment attenuation, or depth gradients thereof, is greatest for softer (clay) sediments. For harder (sand) sediments the sensitivity to attenuation is much decreased. Propagation is most sensitive to the attenuation in the shallowest regions. Thus the degree of sensitivity to attenuation for a particular situation depends most heavily on the extent of shallow regions with soft sediments along the propagation path.

The results of this study also show that neither the local nor the average slope angle are relevant quantities characterizing slope propagation. Instead the length of the shallow water portion of the propagation path is important because that length determines the effect of attenuation. This conclusion holds whenever the adiabatic approximation used in this study is valid, i.e., whenever mode coupling effects can be neglected.

The depth dependence of the sound field and the sensitivity to attenuation is determined by the depth of the deep water element (either source or receiver) and is relatively independent of the shallow water element depth. This holds for either upslope or downslope propagation. Thus the acoustic power versus range, and its partitioning into waterborne or bottom interacting modes, depends on source depth only when the source is in deep water. For upslope propagation the bottom interacting power can be a major component of the acoustic field over a substantial portion of the slope. For downslope propagation at low frequencies of course almost all of the power is bottom interacting in the shallower regions of the slope.

III. A STUDY OF PROPAGATION WITH RANGE VARIABLE BOTTOM ATTENUATION

A. Introduction

This section examines the predictive capabilities of average and locally detailed methods for describing range variable sediment attenuation in shallow water. Inasmuch as the work described in Section II showed that attenuation in shallow water was an important process, this study is also an opportunity to look at the process of sediment attenuation in more detail.

Two problems will be considered. In the absorbing patch problem a comparison is made between a detailed (or localized) sediment attenuation description and a description in which the sediment attenuation is a range average of the detailed dependence. In the second problem this same comparison between detailed and averaged descriptions is made for range varying depth profiles of sediment attenuation.

B. The Absorbing Patch

1. Model Descriptions

Figure 22 shows a sample shallow water environment which was used for a geoacoustic description throughout a region 200 km in extent. The shear and compressional attenuations in the substrate were fixed at 0.03 dB/m/kHz and 0.2 dB/m/kHz, respectively. The sediment attenuation used was determined in two ways. In the model depicted in Fig. 23, one 20 km interval has a sediment attenuation of 0.3 dB/m/kHz, and the remaining 180 km has a sediment attenuation of 0.03 dB/m/kHz. This configuration is called the absorbing patch model. The second configuration had a range invariant sediment attenuation of

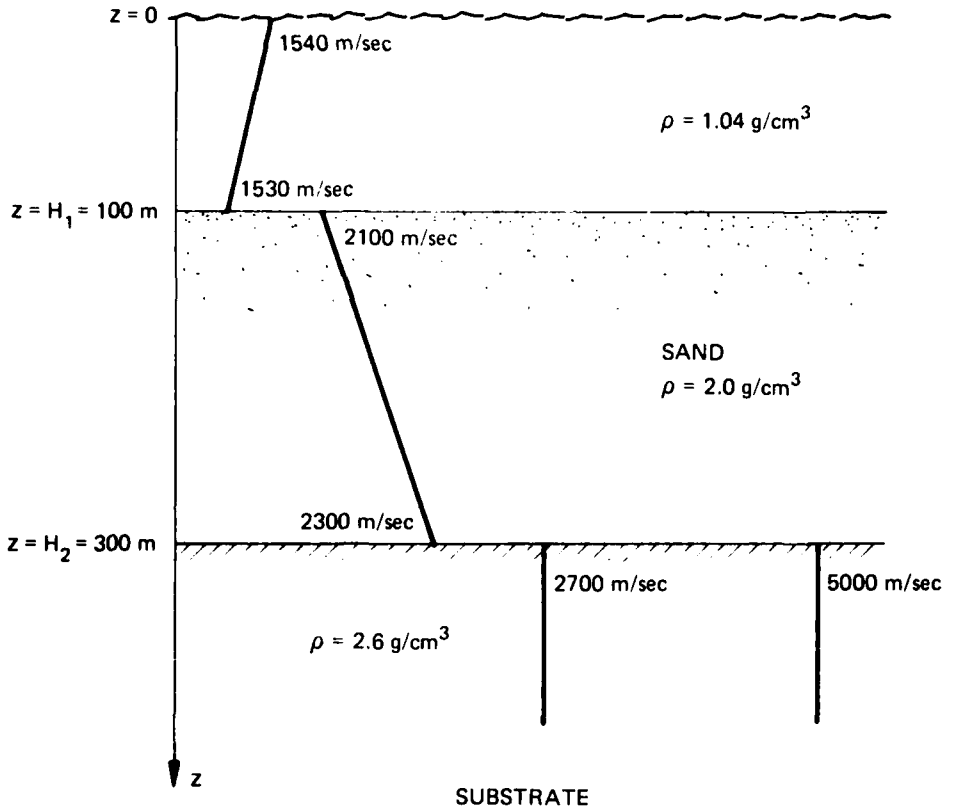

FIGURE 22
SAMPLE OF SHALLOW WATER ENVIRONMENT

ARL:UT
AS-82-186
RAK - GA
3 - 5 - 82

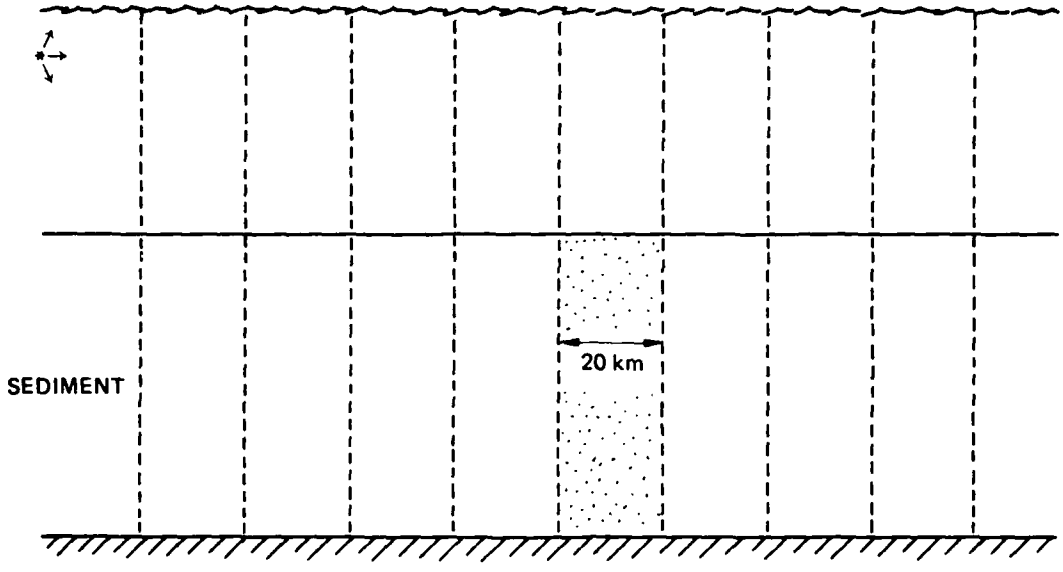

FIGURE 23
ABSORBING PATCH MODEL

ARL:UT
AS-82-187
RAK - GA
3 - 5 - 82

0.057 dB/m/kHz corresponding to the range weighted average of the absorbing patch model.

Given that a mode amplitude decays in range as $\exp\left[-\int_0^r dx\ \delta_n(x)\right]$, where δ_n is the mode attenuation coefficient, then the range averaged attenuation profile is

$$\bar{\alpha}(z) = \int_0^{200\text{km}} dr\ \frac{\alpha(z,r)}{200\ \text{km}} \quad ,$$

where

$$\delta_n(r) = \frac{2\pi f^2}{k_n(r)} \int_0^{\infty} \frac{\alpha(z,r)}{c(z,r)}\ \rho(z)\ \phi_n^2(z,r)\ dz \quad .$$

In this expression for the mode attenuation coefficient, $c(z,r)$ is the sound speed, ρ is the density, ϕ_n is the normal mode depth function, f is the frequency, and k_n is the normal mode eigenvalue (horizontal wave number). To obtain the mode attenuation coefficient δ_n for the range averaged profile, $\bar{\alpha}(z)$ is substituted for the attenuation, $\alpha(z,r)$, in the expression for δ_n. This second configuration is the range averaged model. This proposed definition of range averaged attenuation profile is the only appropriate one for the problem considered because the averaged attenuation coefficient for each mode should reproduce the total modal attenuation obtained from the range variable attenuation coefficient for the averaging interval R. Thus, we require

$$\bar{\delta}_n \equiv \frac{1}{R} \int_0^R dr\ \delta_n(r) \quad .$$

Upon substituting into this equation the previous expression for $\delta_n(r)$ and interchanging the order of range and depth integrations, $\bar{\alpha}(z)$ as defined is seen to be the natural choice for the attenuation profile corresponding to $\bar{\delta}_n$ when no other range variation is present. When the other quantities besides attenuation vary with range, defining an averaged attenuation profile may be less meaningful (see Section IV for related discussion).

2. Results and Comparison

Figure 24 compares the propagation loss versus range for the range averaged model and for the patch model. The patch is located at different positions between source and receiver. The source depth is 10 m and the receiver depth is 100 m. The case with no patch is also shown and gives the upper loss curve, labeled 1, in the figure. When the patch occurs in the first 20 km after the source the propagation loss curve is the lower one, labeled 3 and then 2, in Fig. 24. The range averaged case (curve 4) shows a smooth increase in propagation loss from the no patch curve to the curve for a patch immediately following the source. When the patch is located at some intermediate location, the propagation loss over that range interval smoothly changes from the no patch curve to the curve for a patch immediately following the source (curve 1 to curve 2).

Comparing the two models for treating the range variability in this problem, one finds that either the range averaged or patch method is adequate if no predictions are desired for intermediate ranges. This is seen in Fig. 24 by observing that at 200 km curve 4 for the range averaged profile gives the same incoherent propagation loss as obtained from curve 2 at 200 km. In fact, all of the propagation loss curves obtained by locating the patch center between 10 km and 190 km give the same incoherent propagation loss at 200 km as does curve 2. However, the range averaged description will give substantially misleading results for intermediate ranges. For example, compare curve 3 with curve 4 in Fig. 4. For curve 3, with the patch centered at 10 km, the incoherent propagation loss after 20 km is as much as 7 dB greater than that obtained from curve 4 with the more slowly accumulated loss of the range averaged attenuation profile.

As a practical example, if one is interested in modeling propagation over a variety of paths through a region containing a known sediment channel which passes through an otherwise uniform environment, a patch description will produce a more reliable model result than an

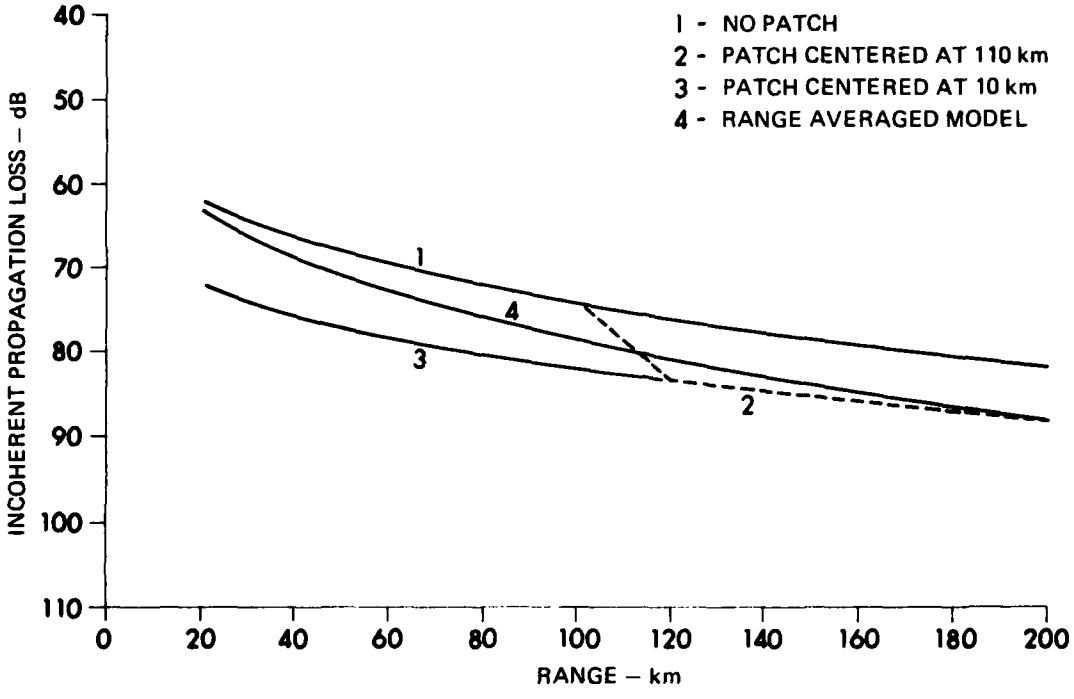

FIGURE 24
PROPAGATION LOSS versus RANGE FOR PATCH AND AVERAGED MODELS
SOURCE DEPTH: 10 m RECEIVER DEPTH: 100 m

ARL:UT
AS-82-188
RAK - GA
3 - 5 - 82

averaged description of the region. On the other hand, because attenuation is cumulative, a propagation problem for which paths always traverse the channel may be solved with either the range averaged or the detailed description.

C. Sensitivity to Attenuation Depth Gradients

1. Model Description

The frequency and geoacoustic parameters used for this problem are the same as those employed in the absorbing patch problem except for the sediment attenuation. In this section a dramatic range variation in the attenuation values and profile is considered. Beginning at the source with a constant sediment attenuation value of 0.03 dB/m/kHz, the attenuation profile smoothly changes to one at 100 km range with a surficial value of 0.3 dB/m/kHz and a constant depth gradient of -0.001 dB/m^2/kHz. Comments on gradient values[12] and results from a problem with a positive gradient are given in Section II.C.6. Between the source and 100 km, the surficial value and the value of the depth gradient change linearly with range. Over the ranges 100-200 km, the attenuation profile smoothly returns to the constant profile used at the source by reversing the change between the source and 100 km. The range average of this sediment attenuation profile is one with a surficial attenuation of 0.165 dB/m/kHz and a constant depth gradient of -0.0005 dB/m^2/kHz. A constant attenuation profile with the same surficial attenuation range variation and the corresponding range average will also be considered.

2. Results and Comparison

Incoherent propagation loss versus range for the range variable and range averaged attenuation profiles is shown in Figs. 25-27 for a source depth of 10 m and receiver depths of 10 m, 50 m, and 100 m, respectively. The results with and without a depth gradient differed by at most a few hundredths of a decibel and are not shown separately.

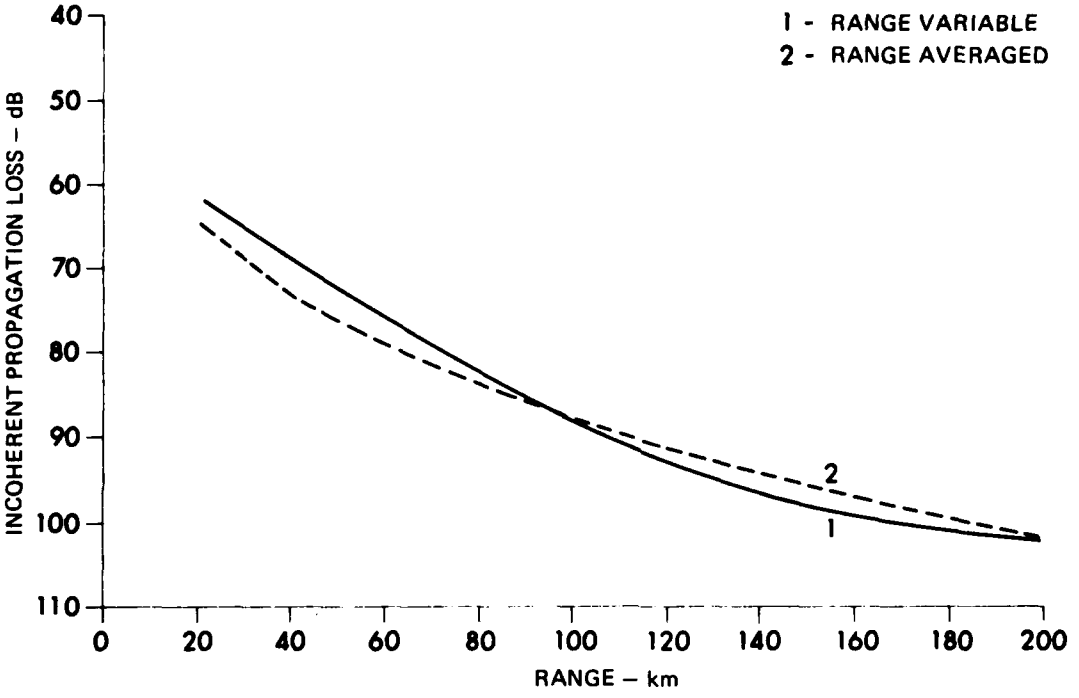

FIGURE 25
PROPAGATION LOSS *versus* RANGE FOR RANGE VARIABLE AND RANGE AVERAGED ATTENUATION PROFILES
SOURCE DEPTH: 10 m RECEIVER DEPTH: 10 m

ARL:UT
AS-82-189
RAK - GA
3 - 5 - 82

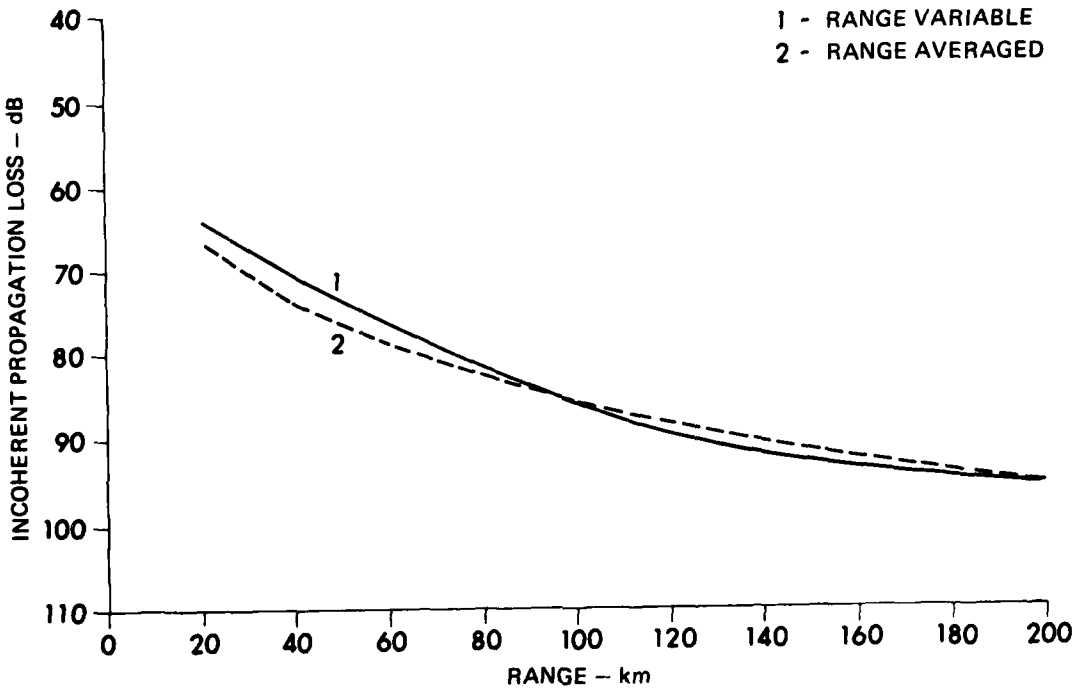

FIGURE 26
PROPAGATION LOSS versus RANGE FOR RANGE VARIABLE AND RANGE AVERAGED ATTENUATION PROFILES
SOURCE DEPTH: 10 m RECEIVER DEPTH: 50 m

ARL:UT
AS-82-190
RAK - GA
3 - 5 - 82

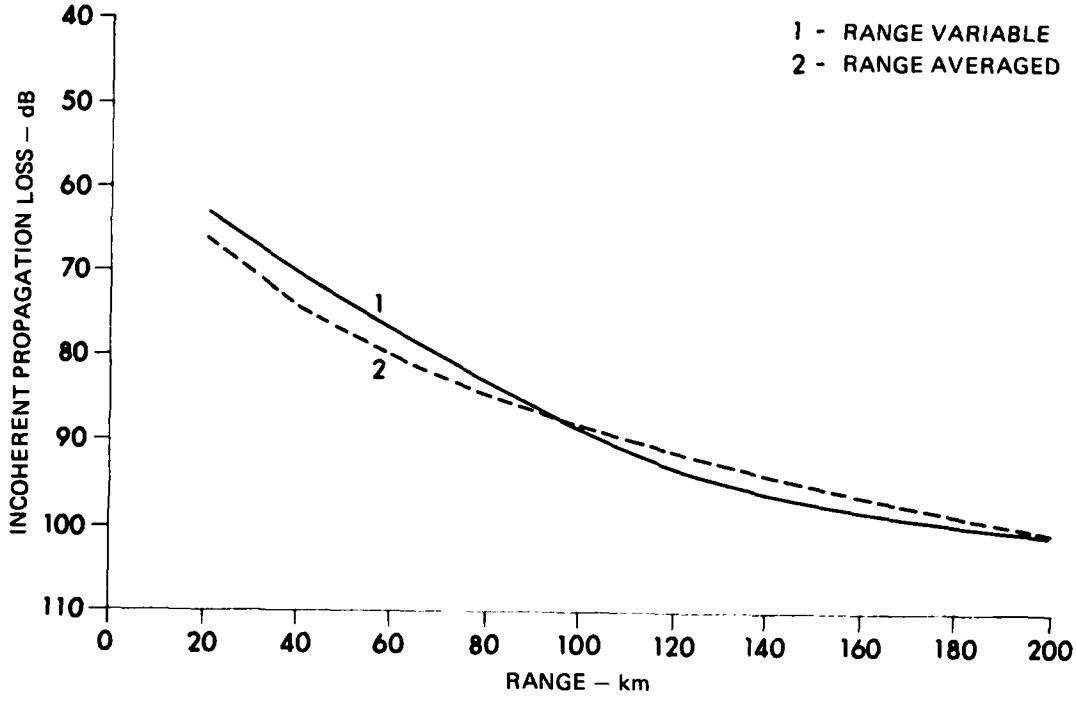

FIGURE 27
PROPAGATION LOSS versus RANGE FOR RANGE VARIABLE AND RANGE AVERAGED ATTENUATION PROFILES
SOURCE DEPTH: 10 m RECEIVER DEPTH: 100 m

ARL:UT
AS-82-191
RAK - GA
3 - 5 - 82

The comparison between range averaged and range variable cases is similar to that in the absorbing patch model. In short, substantial differences in propagation loss between the range averaged and range variable models may occur at ranges interior to the averaging interval.

Before discussing the results of the effect of attenuation depth gradients, several preparatory remarks are appropriate. Hawker et al.[13] discuss the sensitivity to positive attenuation depth gradients typical of various deep water (softer) sediments. The absorption becomes more sensitive to the depth gradient with increasing mode number. The harder sediment and corresponding negative attenuation depth gradient considered here is intended to complement the results of Ref. 13 by treating an appropriate shallow water environment where lateral variability is more common.

The sensitivity shown in Figs. 25-27 to attenuation depth gradients of a physically realistic nature is totally ascribable to the behavior of the mode attenuation coefficients. Because of the large sound speed difference across the water-sediment interface, the first few modes penetrate the bottom only weakly and are slowly attenuated. All the remaining modes, with horizontal phase velocities exceeding the sound speed at the top of the sediment layer, are heavily attenuated due to stronger penetration and interaction with the bottom. Thus, the modes which propagate with the least attenuation barely sample the depth dependence of the attenuation while the modes which do sample the attenuation depth dependence are quickly attenuated in range. The long range sound field is thus dominated by the least attenuated modes which are least sensitive to the attenuation depth gradient.

For softer sediments, a greater sensitivity to the attenuation depth gradient is likely to occur (as was observed in Section II.C.6) because the sound field will better penetrate the sediment and sample more than the surficial attenuation. However, even for softer sediments the sensitivity to the attenuation gradient is likely to vary with increasing range and for the reason cited in Section II.C.6. The

shallower the water the more rapid the change in sensitivity with range. With respect to the loss versus range for a sediment with a constant attenuation value equal to the surficial value when a gradient is present, the propagation loss with a negative gradient in sediment attenuation will first decrease when the higher order modes are more slowly attenuated deep in the sediment than with no gradient. As these higher order modes become, at longer ranges, more attenuated and less important than the lower order modes, the propagation loss with the gradient approaches the loss without the gradient. Eventually, at the longest ranges the loss with the negative gradient decreases relative to the loss with no gradient.

A negative gradient in the attenuation profile is also probably less noticeable than a positive gradient. Modes which penetrate the sediment far enough to notice the negative gradient are still as heavily attenuated in the near-surface sediment as less penetrating modes, whereas modes which penetrate into a positive gradient would be more heavily attenuated than modes which do not penetrate.

IV. LATERAL VARIABILITY ON A SLOPING BOTTOM

On continental slopes and margins some variability in sediment types is expected. As observed in Section II, different sediment types vary in the degree to which propagation is sensitive to their attenuation values. In order to establish priorities for measuring the geoacoustic parameters of these sloping bottom areas several factors need to be taken into account. The importance of the shallow water end of the slope has clearly been established as has the need for accurate sediment attenuation values in that region. The implication is that the priority for establishing sediment properties decreases with increasing water depth along the slope. Thus, removing uncertainties in bottom type in the deeper regions of a slope has a lower priority than obtaining the properties of the more shallow portions of the slope.

To illustrate this point consider the problem of modeling propagation for the 3^{0} upslope geometry with sediment parameters described in Section II, except for an attenuation gradient in the sediment as given in Section II.C.6. Instead of using the same sediment type throughout, let the deep water range interval comprising the first 40 km have either a sand, silt, or clay sediment. A clay sediment is used over the remainder of the range interval. Thus, by comparing the incoherent propagation loss versus range for the three different sediment types used in the deep water the relative importance for upslope propagation of knowledge of the deep water sediments to knowledge of the shallow water sediments may be ascertained.

Figures 28-31 show the results of this study. For all four source depth/receiver depth combinations the propagation loss through the deep water regions (first 40 km) is quite different for the three sediment

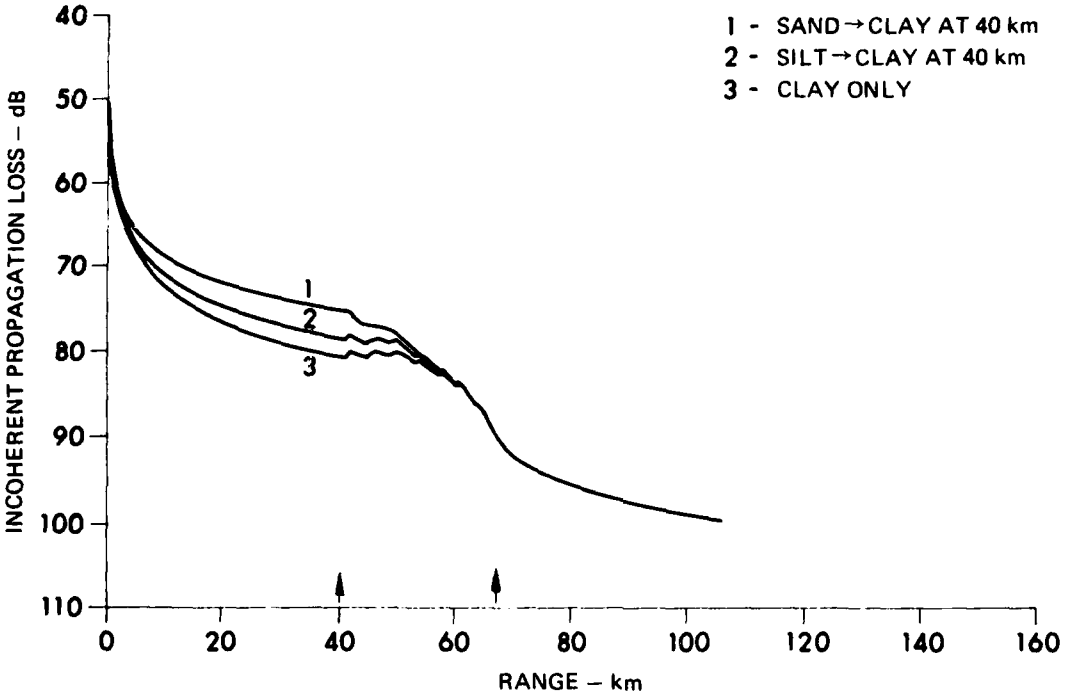

FIGURE 28
PROPAGATION LOSS versus RANGE FOR LATERALLY VARYING SEDIMENT ON A SLOPE

SOURCE DEPTH: 18 m RECEIVER DEPTH: 18 m
SEDIMENT ATTENUATION: 0.025 dB/m/kHz to 0.2 dB/m/kHz in 200 m
BOTTOM SLOPE: 3° UP

ARL:UT
AS-82-192
RAK - GA
3 - 5 - 82

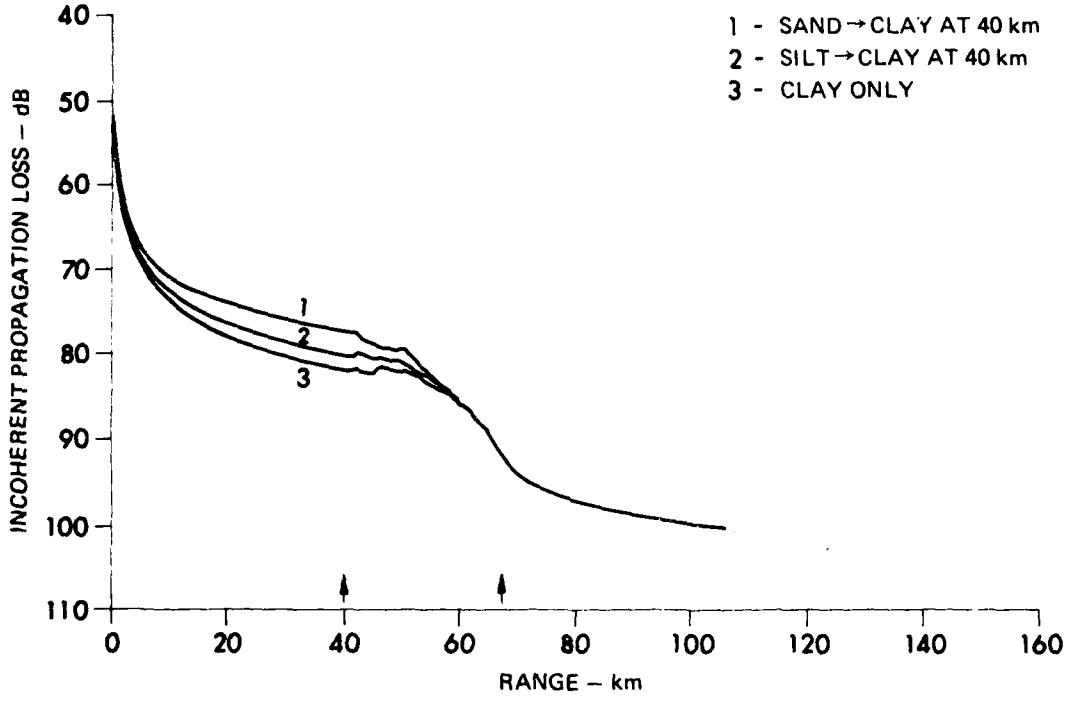

FIGURE 29
PROPAGATION LOSS versus RANGE FOR LATERALLY VARYING SEDIMENT ON A SLOPE

SOURCE DEPTH: 18 m RECEIVER DEPTH: 91 m
SEDIMENT ATTENUATION: 0.025 dB/m/kHz to 0.2 dB/m/kHz in 200 m
BOTTOM SLOPE: 3° UP

ARL:UT
AS-82-193
RAK - GA
3 - 5 - 82

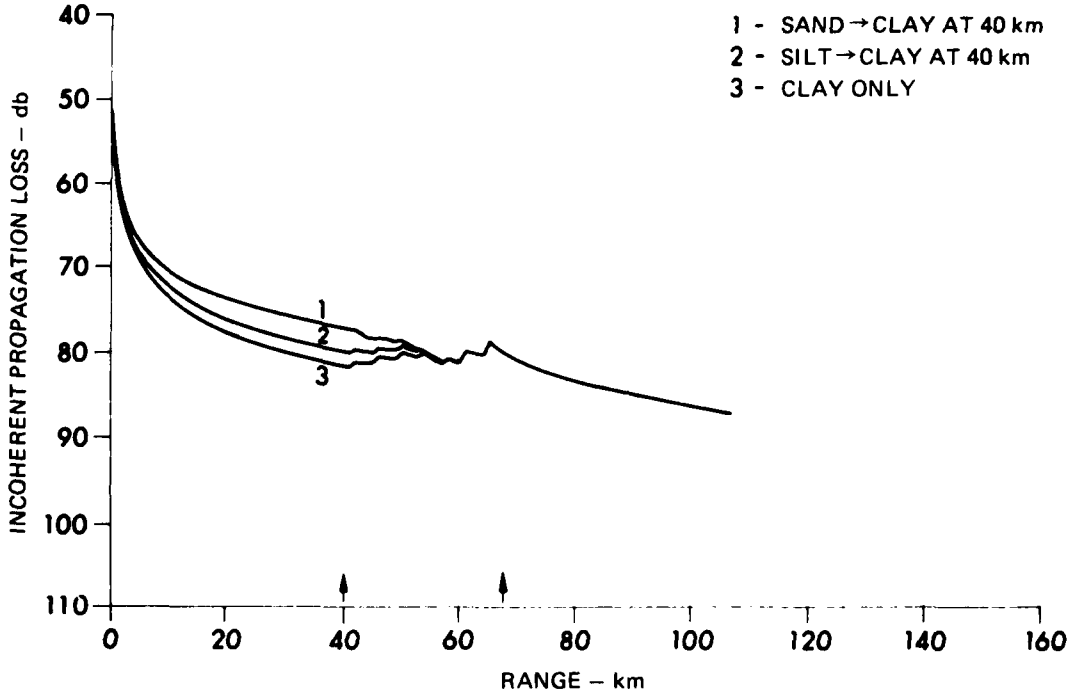

FIGURE 30
PROPAGATION LOSS versus RANGE FOR LATERALLY VARYING SEDIMENT ON A SLOPE
SOURCE DEPTH: 91 m RECEIVER DEPTH: 18 m
SEDIMENT ATTENUATION: 0.025 dB/m/kHz to 0.2 dB/m/kHz in 200 m
BOTTOM SLOPE: 3° UP

ARL:UT
AS-82-194
RAK - GA
3 - 5 - 82

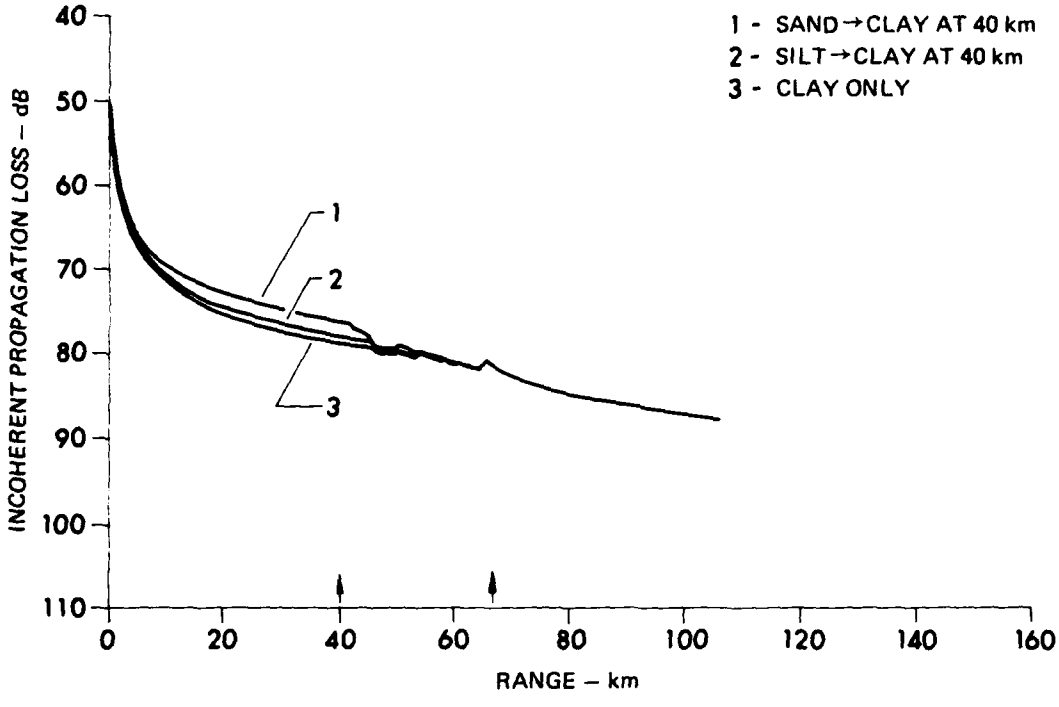

FIGURE 31
PROPAGATION LOSS versus RANGE FOR LATERALLY VARYING SEDIMENT ON A SLOPE

SOURCE DEPTH: 91 m RECEIVER DEPTH: 91 m
SEDIMENT ATTENUATION: 0.025 dB/m/kHz to 0.2 dB/m/kHz in 200 m
BOTTOM SLOPE: 3° UP

ARL:UT
AS-82-195
RAK - GA
3 - 5 - 82

types. However, as the clay sedimented slope is traversed, the three incoherent propagation loss curves merge in each figure some 10 km before the top of the slope where the sound channel axis intersects the water-sediment interface. The coherent propagation loss curves also merge eventually, but they do not become especially similar until approximately 10 km into the shallow water past the edge of the slope.

One aspect of these results that should be noted is that, consistent with the results discussed in Section II and in Ref. 9, the variation in propagation loss over the first 40 km for the three different sediments is dependent upon source depth, i.e., the differences result because the highest order modes to which a shallow source couples are most sensitive to bottom type. Thus, bottom type is not negligible in determining the sound field incident on the slope, especially for either shallow sources or receivers. Also, the effect of bottom type could not be neglected if propagation between near-surface or near-bottom sources and receivers in deep water were the subject of interest.

Because the modeling parameters in this example were somewhat exaggerated, some care must be exercised in drawing conclusions. Indeed, additional work in this area is needed. However, our conclusion concerning the relative importance of the shallow water parameters are well founded because they are based upon knowledge of the relevant propagation mechanisms.

A tentative conclusion is that a more detailed description of the continental margins is more suitable for propagation modeling of slopes than an "average" bottom description because of the rapid change in sensitivity to bottom parameters as sound propagates over a slope.

V. CONCLUSIONS

The work presented in this report concerns the propagation of low frequency underwater sound over regions with sloping bottoms and laterally varying subbottom properties.

The work in Section II considered low frequency underwater acoustic propagation over thickly sedimented slopes. The major propagation mechanisms identified were spreading loss, renormalization, bottom attenuation, mode effectiveness, and mode cutoff. Bottom type, SVP, and water depth are environmental features which determine the relative importance of these propagation mechanisms. In determining the relative importance of these mechanisms, the effect of varying range, source depth, receiver depth, sediment type, sediment attenuation, bottom slope, and sediment attenuation gradient was studied. The role of basement properties, sediment thickness, shallow water depth and SVP, and frequency was not treated.

The following conclusions were reached concerning propagation over a sloping bottom.

1. The sensitivity of incoherent propagation loss to the value of sediment attenuation increases with changes in sediment type from sand to silt to clay. However, when the magnitude of attenuation value is restricted to the physical range appropriate to each sediment type, this sensitivity is approximately independent of sediment type. This happens because the increase in sensitivity with sediment type is compensated for by a decreasing physical range of variability for attenuation values.

2. Accurate values of sediment attenuation are more important for shallow water than deep water. This relative importance increases with increasing difference in water depth between deep and shallow areas.

3. The relative importance of using accurate shallow water sediment attenuation values versus accurate deep water sediment attenuation values increases with increasing range from the shallow water acoustic element to the beginning of the slope.

4. Slope angle is not a useful parameter for characterizing incoherent propagation loss over thickly sedimented slopes. All effects ascribable to slope angle are more usefully decomposed into cylindrical spreading and accumulated attenuation.

5. Incoherent propagation loss for propagation over slopes depends on the depth of the deep water element only, whether it be the source (upslope) or receiver (downslope). It depends only weakly on the depth of the shallow water element. The depth gradient of the downslope incoherent propagation loss is strongest near the water surface or near the water-sediment interface. This depth gradient is weakest near the sound channel axis.

6. The ratio of bottom interacting power to waterborne power from deep water sources increases as the source moves nearer the surface and away from the sound channel. As the source depth approaches the channel axis, the waterborne power nearer the channel axis is converted upon encountering a slope into bottom interacting power which is less rapidly attenuated than the bottom interacting power propagating directly from sources nearer the water surface.

7. The sensitivity of propagation to positive sediment attenuation gradients may increase or decrease with source to receiver separation. This sensitivity will typically decrease with increasing range for propagation to short ranges in either deep or shallow water or downslope. For upslope propagation or at sufficiently long ranges in

shallow water, the effect of a sediment attenuation gradient will typically increase with increasing range.

The work in Section III considered low frequency shallow water propagation over thick sand sediments with laterally varying attenuation. A comparison was made between range averaged and unaveraged descriptions of an absorbing sediment patch and of a range varying attenuation gradient. The following conclusions were made.

1. For propagation over ranges different from that over which the averaging was performed, the range averaged description of lateral sediment variations can give large errors in incoherent propagation loss.

2. For a fixed low frequency, incoherent propagation loss over thick sand sediments in shallow water is insensitive to modest negative depth gradients in the attenuation profile.

The work in Section IV considered low frequency propagation up a slope with thick sediment cover and laterally varying sediment type. The following conclusion was made.

1. The importance of deep water sediment type in determining the incoherent propagation loss decreases with range from the bottom to the top of the slope.

Several observations are relevant with regard to various aspects of this work. Questions concerning the sensitivity of a quantity, such as propagation loss, to variations in parameters can have meaningful answers if the questions specify how the quantity is to be used. For example, suppose a system performance prediction will be accurate if an uncertainty of 0.05 dB/m/kHz in the sediment attenuation value produces less than 3 dB change in propagation loss. Results presented here show that for silt and clay this requirement is not met, whereas for sand it is. In this instance propagation over silt and clay would be sensitive

to variations in sediment attenuation values whereas propagation over sand would not be. On the other hand, if accurate system performance predictions require that any value from the observed range of attenuations for a given sediment give the same propagation loss prediction within 3 dB, then propagation over any sediment type would be sensitive to sediment attenuation value because the requirement is not met for any sediment, as shown by the results presented here. Conversely, the same results show that measurement of propagation loss to within 3 dB might allow the determination of attenuation value for a clay sediment to within 0.03 dB/m/kHz, whereas the same measurement for a sand sediment could give an uncertainty of 0.1 dB/m/kHz or larger. Similar comments could be made concerning the results of Sections III and IV on sensitivity to lateral variations.

Since the time the work on sensitivity to depth gradients of sediment attenuation was performed, as reported in Section III, Mitchell and Focke[14] have observed that the existence of an optimum frequency for shallow water propagation may be related to the behavior of the attenuation profile with depth. Inasmuch as the lateral variability study results given in Section III do not consider frequency dependence, future efforts should be directed to this aspect of the problem.

Another area for future work in lateral variability is the further examination of propagation over variable sediment type, particularly in more shallow regions of a slope. The effect of sediment patching on coherence between array elements would be of interest.

Finally, future efforts need to examine the effect of solid basements and sediments in propagation through range variable environments. The additional mechanisms associated with shear waves should be identified, especially for propagation over sloping bottoms with sediment variability.

ACKNOWLEDGMENTS

Dr. P. J. Vidmar's comments and suggestions in the course of this work and on this manuscript are gratefully acknowledged. Dr. S. K. Mitchell's suggestions concerning the absorbing patch model are also appreciated.

REFERENCES

1. K. E. Hawker, S. R. Rutherford, and P. J. Vidmar, "A Summary of the Results of a Study of Acoustic Interaction with the Sea Floor," Applied Research Laboratories Technical Report No. 79-2 (ARL-TR-79-2) Applied Research Laboratories, The University of Texas at Austin, 5 March 1979.

2. A. D. Pierce, "Extension of the Method of Normal Modes to Sound Propagation in an Almost-Stratified Medium," J. Acoust. Soc. Am. 37, 19-27 (1965).

3. D. M. Milder, "Ray and Wave Invariants for SOFAR Channel Propagation," J. Acoust. Soc. Am. 46, 1259-1263 (1969).

4. S. R. Rutherford, "An Examination of Coupled Mode Theory as Applied to Underwater Sound Propagation," Applied Research Laboratories Technical Report No. 79-44 (ARL-TR-79-44), Applied Research Laboratories, The University of Texas at Austin, 26 July 1979.

5. S. R. Rutherford and K. E. Hawker, "A Consistent Coupled Mode Theory of Sound Propagation for a Class of Nonseparable Problems," J. Acoust. Soc. Am. 70, 554-564 (1981).

6. S. R. Rutherford, "An Examination of Multipath Processes in a Range Dependent Ocean Environment within the Context of Adiabatic Mode Theory," J. Acoust. Soc. Am. 66, 1482-1486 (1979).

7. S. R. Rutherford and K. E. Hawker, "An Examination of the Influence of the Range Dependence of the Ocean Bottom on the Adiabatic Approximation," J. Acoust. Soc. Am. 66, 1145-1151 (1979).

8. P. J. Vidmar, S. R. Rutherford, and K. E. Hawker, "A Summary of Some Recent Results in Acoustic Bottom Interaction," Applied Research Laboratories Technical Report No. 80-6 (ARL-TR-80-6), Applied Research Laboratories, The University of Texas at Austin, 19 February 1980.

9. S. R. Rutherford, S. G. Payne, and R. A. Koch, "A Summary of the Results of a Study of Acoustic Bottom Interaction in a Range Dependent Environment," Applied Research Laboratories Technical Report No. 80-56 (ARL-TR-80-56), Applied Research Laboratories, The University of Texas at Austin, 14 November 1980.

10. P. J. Vidmar, R. A. Koch, J. F. Lynch, and K. E. Hawker, "A Summary of Recent Results in Acoustic Bottom Interaction Research," Applied Research Laboratories Technical Report No. 81-11 (ARL-TR-81-11), Applied Research Laboratories, The University of Texas at Austin, 24 March 1981.

11. E. L. Hamilton, "Prediction of Deep-Sea Sediment Properties: State-of-the-Art," in Deep Sea Sediments, Physical and Mechanical Properties, A. L. Inderbitzen, ed. (Plenum Press, New York, 1974), pp. 1-43.

12. E. L. Hamilton, "Sound Attenuation as a Function of Depth in the Sea Floor," J. Acoust. Soc. Am. 59, 528-535 (1976).

13. K. E. Hawker, W. E. Williams, and T. L. Foreman, "A Study of the Acoustical Effects of Subbottom Absorption Profiles," J. Acoust. Soc. Am. 65, 360-367 (1979).

14. S. K. Mitchell and K. C. Focke, "The Role of the Sea-Bottom Attenuation Profile in Shallow Water Acoustic Propagation" (in preparation).

1 June 1982

DISTRIBUTION LIST FOR
ARL-TR-82-30
UNDER CONTRACT N00014-78-C-0113
UNCLASSIFIED

Copy No.

Commanding Officer
Naval Ocean Research and Development Activity
NSTL Station, MS 39529
1 Attn: E. D. Chaika (Code 530)
2 W. A. Kuperman (Code 320)
3 CDR M. McCallister (Code 520)
4 J. Matthews (Code 360)
5 G. Morris (Code 340)
6 W. W. Worsley (Code 530)

Commanding Officer
Office of Naval Research
Arlington, VA 22217
7 Attn: P. Rogers (Code 425AC)
8 J. M. McKisic (Code 425AC)
9 G. Johnson (Code 428AR)

10 Office of Naval Research
Branch Office, Chicago
Department of the Navy
536 South Clark Street
Chicago, IL 60605

Commanding Officer
Naval Electronic Systems Command
Washington, D.C. 20360
11 Attn: LCDR S. Hollis (Code 612)
12 CDR C. Spikes (PME 124-60)
13 CDR P. Girard (PME 612)

Director
Naval Research Laboratory
Department of the Navy
Washington, D.C. 20375
14 Attn: B. B. Adams (Code 8160)
15 W. Mosley
16 O. Diachok
17 F. Ingenito

Distribution List for ARL-TR-82-30 under Contract N00014-78-C0113 (Cont'd)

Copy No.

Commanding Officer
Naval Ocean Systems Center
Department of the Navy
San Diego, CA 92152
18 Attn: E. L. Hamilton
19 M. A. Pederson
20 H. P. Bucker
21 R. Bachman

Commander
Naval Sea System Command
Department of the Navy
Washington, D.C. 20362
22 Attn: R. W. Farwell (Code 63RA)

Chief of Naval Operations
Department of the Navy
Washington, D.C. 20350
23 Attn: CDR J. Harlette (OP 952D)

Chief of Naval Material
Department of the Navy
Washington, D.C. 20360
24 ATTN: CAPT E. Young (MAT 08T245)

25 Commander
Naval Surface Weapons Center
White Oak Laboratory
Department of the Navy
Silver Spring, MD 20910

26 Commander
David W. Taylor Naval Ship Research and Development Center
Department of the Navy
Bethesda, MD 20034

Naval Oceanographic Office
Department of the Navy
NSTL Station, MS 39529
27 Attn: W. Jobst (Code 3400)
28 M. G. Lewis (Code 7200)
29 J. Allen

Distribution List for ARL-TR-82-30 under Contract N00014-78-C-0113 (Cont'd)

Copy No.

Commander
Naval Air Development Center
Department of the Navy
Warminister, PA 18974
30 Attn: C. L. Bartberger

Officer in Charge
New London Laboratory
Naval Underwater Systems Center
Department of the Navy
New London, CT 06320
31 Attn: B. Cole
32 F. R. DiNapoli
33 D. Lee

34 Director Naval Warfare
Deputy Undersecretary of Defense, R&E
Room 3D1048, Pentagon
Washington, D.C. 20301

OASN (R,E&S)
Room 4D745, Pentagon
Washington, D.C. 20301
35 Attn: G. A. Cann

Superintendent
Naval Postgraduate School
Monterey, CA 93940
36 Attn: Library

Commander
Naval Coastal Systems Center
Department of the Navy
Panama City, FL 32407
37 Attn: G. McLeroy

38- 49 Commanding Officer and Director
Defense Information Service Center
Cameron Station, Building 5
5010 Duke Street
Alexandria, VA 22314

Defense Advanced Research Projects Agency
1400 Wilson Blvd.
Arlington, VA 22209
50 Attn: CDR K. Evans (TTO)

Distribution List for ARL-TR-82-30 under Contract N00014-78-C-0113 (Cont'd)

Copy No.

51 Commander
Naval Intelligence Support Center
4301 Suitland Road
Washington, D.C. 20390

Woods Hole Oceanographic Institution
86-95 Water Street
Woods Hole, MA 02543
52 Attn: E. E. Hayes
53 R. Spindel

Science Applications, Inc.
1710 Goodridge Drive
McLean, VA 22101
54 Attn: J. Hanna
55 L. Dozier

Applied Research Laboratory
The Pennsylvania State University
P. O. Box 30
State College, PA 16801
56 Attn: S. McDaniel

Marine Physical Laboratory of
The Scripps Institution of Oceanography
The University of California, San Diego
San Diego, CA 92132
57 Attn: F. Fisher
58 G. Shor

Scripps Institution of Oceanography
The University of California, San Diego
La Jolla, CA 92037
59 Attn: Library
60 R. Tyce

Bell Telephone Laboratories, Inc.
Whippany Road
Whippany, NJ 07961
61 Attn: S. A. Kramer

Planning Systems, Inc.
7900 Westpark Drive, Suite 507
McLean, VA 22101
62 Attn: R. Cavanaugh

Distribution List for ARL-TR-82-30 under Contract N00014-78-C-0113 (Cont'd)

Copy No.

TRW, Inc.
TRW Electronics and Defense Sector
Systems Engineering and Applications Division
7600 Colshire Drive
McLean, VA 22101
63 Attn: R. T. Brown

Defence Scientific Establishment
HMNZ Dockyard
Devonport, Auckland
NEW ZEALAND
64 Attn: K. M. Guthrie

School of Mechanical Engineering
Georgia Institute of Technology
Atlanta, GA 30332
65 Attn: A. D. Pierce

Department of Geology and Geophysics
Geophysical and Polar Research Center
Lewis G. Weeks Hall for Geological Sciences
The University of Wisconsin, Madison
1215 W. Dayton Street
Madison, WI 53706
66 Attn: C. S. Clay

Courant Institute
251 Mercer Street
New York, NY 10012
67 Attn: D. C. Stickler

Bolt, Beranek, & Newman, Inc.
50 Moulton Street
Cambridge, MA 02138
68 Attn: H. Cox

Hawaii Institute of Geophysics
The University of Hawaii
2525 Correa Road
Honolulu, HI 96822
69 Attn: G. Sutton
70 L. N. Frazer

Distribution List for ARL-TR-82-30 under Contract N00014-78-C-0113 (Cont'd)

Copy No.

Director
North Atlantic Treaty Organization
SACLANT ASW Research Centre
APO New York 09019
71 Attn: T. Akal
72 F. Jensen
73 R. Wagstaff

Defence Research Establishment Pacific
CF Dockyard
Victoria, BC
CANADA
74 Attn: R. Chapman

Defence Research Establishment Atlantic
9 Grove Street
P. O. Box 1012
Dartmouth, NS
CANADA
75 Attn: D. Chapman

Rosenteil School of Marine and
Atmospheric Science
The University of Miami
10 Rickenbacker Causeway
Miami, FL 33149
76 Attn: H. DeFarrari
77 F. Tappert

Applied Physics Laboratory
The Johns Hopkins University
Johns Hopkins Road
Laurel, MD 20810
78 Attn: J. Lombardo

Department of Physics
The University of Rhode Island
Kingston, RI 02881
79 Attn: C. Kaufman

Department of Electrical Engineering
Polytechnic Institute of New York
Farmingdale, NY 11735
80 Attn: L. B. Felsen

81 I. Tolstoy
Knockvennie, Castle Douglas
S. W. SCOTLAND
GREAT BRITAIN

Distribution List for ARL-TR-82-30 under Contract N00014-78-C-0113 (Cont'd)

Copy No.

Department of Geology
The University of Texas at Austin
Austin, TX 78712
82 Attn: C. Wilson

Department of Physics
The University of Auckland
Private Bag, Auckland
NEW ZEALAND
83 Attn: A. C. Kibblewhite
84 C. T. Tindle

Brown University
Providence, RI 02912
85 Attn: A. O. Williams, Jr.

The Lamont-Doherty Geological Observatory
Columbia University
Palisades, NY 10964
86 Attn: R. D. Stoll
87 H. Kutschale

Western Electric Company, Inc.
P. O. Box 20046 - GC7420
Greensboro, NC 27420
88 ATTN: T. Clark

89 Office of Naval Research
Resident Representative
Room No. 582, Federal Building
Austin, TX 78701

90 Environmental Sciences Division, ARL:UT

91 Terry L. Foreman, ARL:UT

92 Robert F. Gragg, ARL:UT

93 Loyd Hampton, ARL:UT

94 Kenneth E. Hawker, ARL:UT

95 Robert A. Koch, ARL:UT

96 Jo Lindberg, ARL:UT

97 Stephen K. Mitchell, ARL:UT

Distribution List for ARL-TR-82-30 under Contract N00014-78-C-0113 (Cont'd)

Copy No.

98	Clark S. Penrod, ARL:UT
99	Paul J. Vidmar, ARL:UT
100	Reuben H. Wallace, ARL:UT
101	Library, ARL:UT
102 - 112	Reserve, ARL:UT


DATE
ILME